

Modes

in Classical and Quantum Optics

Claude Fabre

Covariance Matrix

single mode case :

$$\begin{bmatrix} \Delta^2 E_{X1} & C(E_{X1}E_{Y1}) \\ C(E_{Y1}E_{X1}) & \Delta^2 E_{Y1} \end{bmatrix}$$

two-mode case:

$$\begin{bmatrix} \Delta^2 E_{X1} & C(E_{X1}E_{X2}) & C(E_{X1}E_{Y1}) & C(E_{X1}E_{Y2}) \\ C(E_{X2}E_{X1}) & \Delta^2 E_{X2} & C(E_{X2}E_{Y1}) & C(E_{X2}E_{Y2}) \\ C(E_{Y1}E_{X1}) & C(E_{Y1}E_{X2}) & \Delta^2 E_{Y1} & C(E_{Y1}E_{Y2}) \\ C(E_{Y2}E_{X1}) & C(E_{Y2}E_{X2}) & C(E_{Y2}E_{Y1}) & \Delta^2 E_{Y2} \end{bmatrix}$$

symmetric, positive matrix, therefore diagonalizable

"principal component analysis"

Recherche de modes propres: cas mono-quadrature et N modes

$$\begin{bmatrix} \Delta^2 E_{X1} & C(E_{X1}E_{X2}) & \dots & C(E_{X1}E_{XN}) \\ C(E_{X2}E_{X1}) & \Delta^2 E_{X2} & \dots & C(E_{X2}E_{XN}) \\ \dots & \dots & \dots & \dots \\ C(E_{XN}E_{X1}) & C(E_{XN}E_{X2}) & \dots & \Delta^2 E_{XN} \end{bmatrix}$$

généralisable à N modes: N modes propres existent

$$\begin{bmatrix} \Delta^2 E_{X'1} & 0 & 0 & 0 \\ 0 & \Delta^2 E_{X'2} & 0 & 0 \\ \dots & \dots & \dots & \dots \\ 0 & 0 & 0 & \Delta^2 E_{X'N} \end{bmatrix}$$



Measuring the Transmission Matrix in Optics: An Approach to the Study and Control of Light Propagation in Disordered Media

S. M. Popoff, G. Lerosey, R. Carminati, M. Fink, A. C. Boccara, and S. Gigan

Institut Langevin, ESPCI ParisTech, CNRS UMR 7587, ESPCI, 10 rue Vauquelin, 75005 Paris, France
(Received 27 October 2009; revised manuscript received 11 January 2010; published 8 March 2010)

We introduce a method to experimentally measure the monochromatic transmission matrix of a complex medium in optics. This method is based on a spatial phase modulator together with a full-field interferometric measurement on a camera. We determine the transmission matrix of a thick random scattering sample. We show that this matrix exhibits statistical properties in good agreement with random matrix theory and allows light focusing and imaging through the random medium. This method might give important insight into the mesoscopic properties of a complex medium.

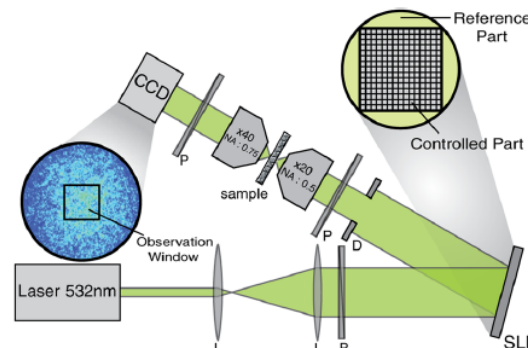
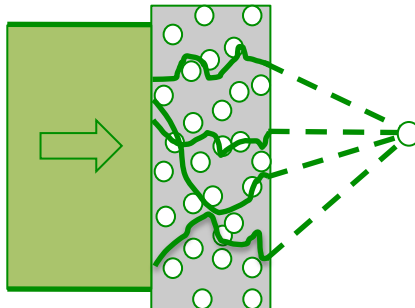


FIG. 1 (color online). Schematic of the apparatus. The laser is expanded and reflected off a SLM. The phase-modulated beam is focused on the multiple-scattering sample and the output intensity speckle pattern is imaged by a CCD camera: lens (L), polarizer (P), diaphragm (D).

Transmission through scattering medium

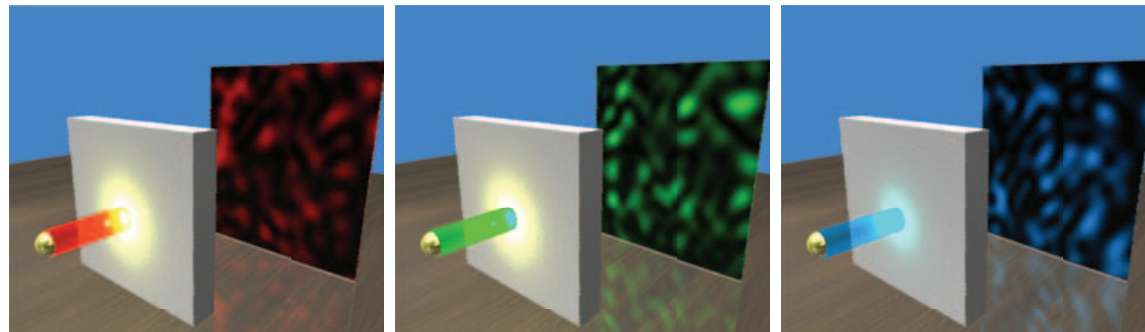
Monochromatic speckle



A speckle grain =

- Sum of different paths with random phases
 $= \text{random walk in the complex plane}$
- Size limited by diffraction
- Intensity distribution $R(I) \propto \exp^{-I/\langle I \rangle}$
- unpolarized speckle = 2 independent speckles

Polychromatic (i.e. temporal)

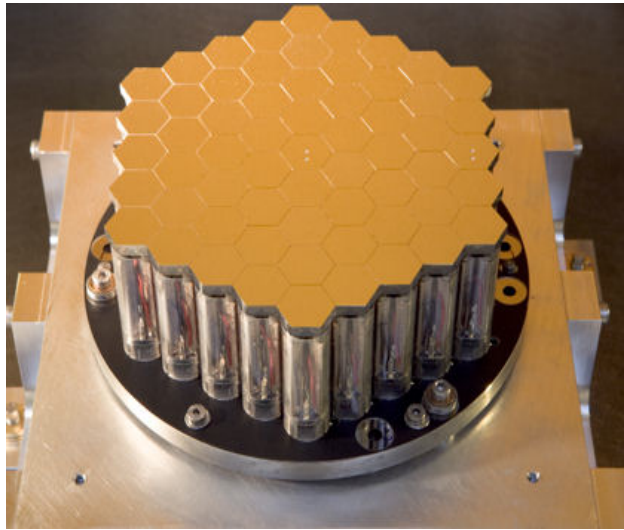


Mosk et al. Nature Photonics May 2012

Spectral dependence/
confinement time of
light in the medium

Speckle figure : complex distribution ... but **coherent** and **deterministic**

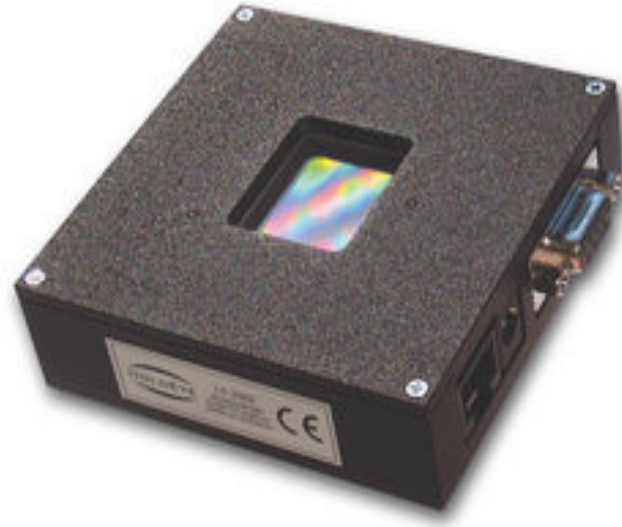
Device for wavefront control



Deformable mirrors
(piezo, magnetics...)

10-100 actuators (typ.)
course : 10-20 microns
Speed > kHz

Adaptive optics



Spatial light modulator (SLM)
(mostly liquid crystals)

Segmented, >1 million pixel
course : 1 microns
speed: <50Hz

Diffractive optics, displays ...

Transmission matrix measurement and use

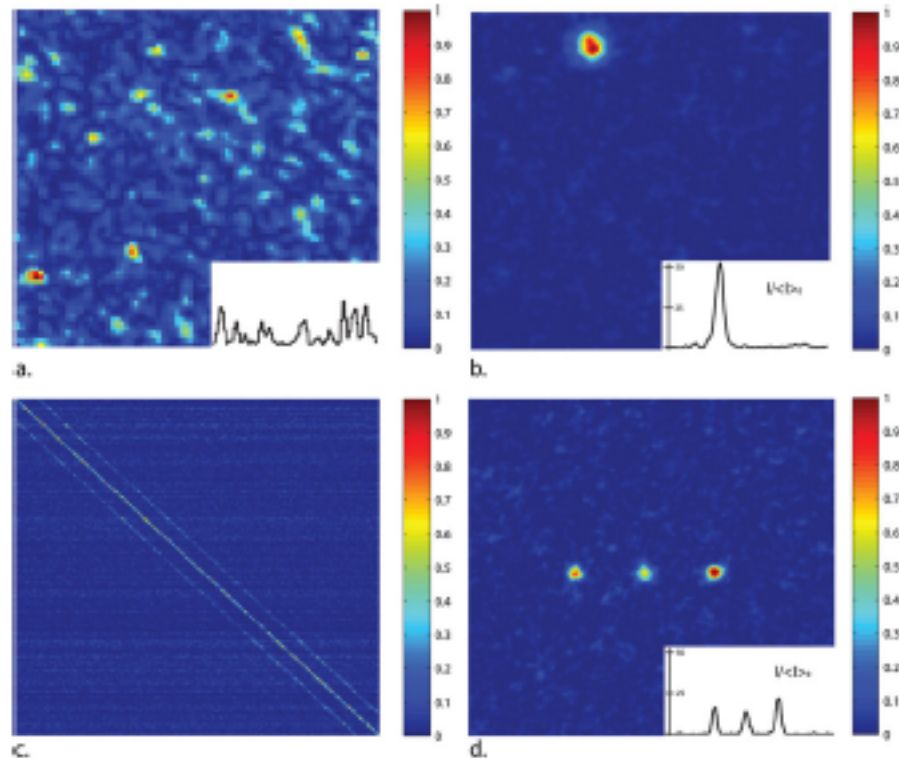


FIG. 2 (color online). Experimental results of focusing.
(a) Initial aspect of the output speckle. (b) We measure the TM for 256 controlled segments and use it to perform phase conjugation. (c) Norm of the focusing operator $O_{\text{norm}}^{\text{foc}}$.
(d) Example of focusing on several points. (The insets show intensity profiles along one direction.)

singular value decomposition of the transmission matrix
valid for any matrix

$$M = U \cdot \text{diag}(\lambda) \cdot V \quad U, V \text{ unitaries}$$

histogram
of singular values

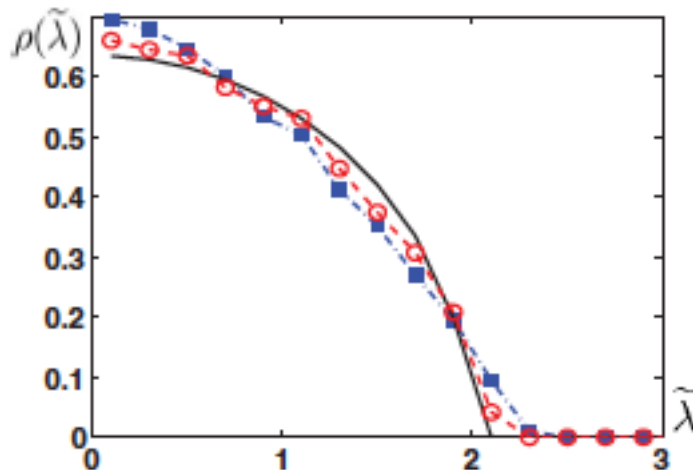


FIG. 4 (color online). Singular value distribution of the experimental transmission matrices obtained by averaging over 16 realizations of disorder. The solid line is the quarter-circle law predicted for random matrices. With the solid squares the matrix filtered to remove the reference amplitude contribution and with the circles the matrix obtained by filtering and removing neighboring elements to eliminate interelement correlations.

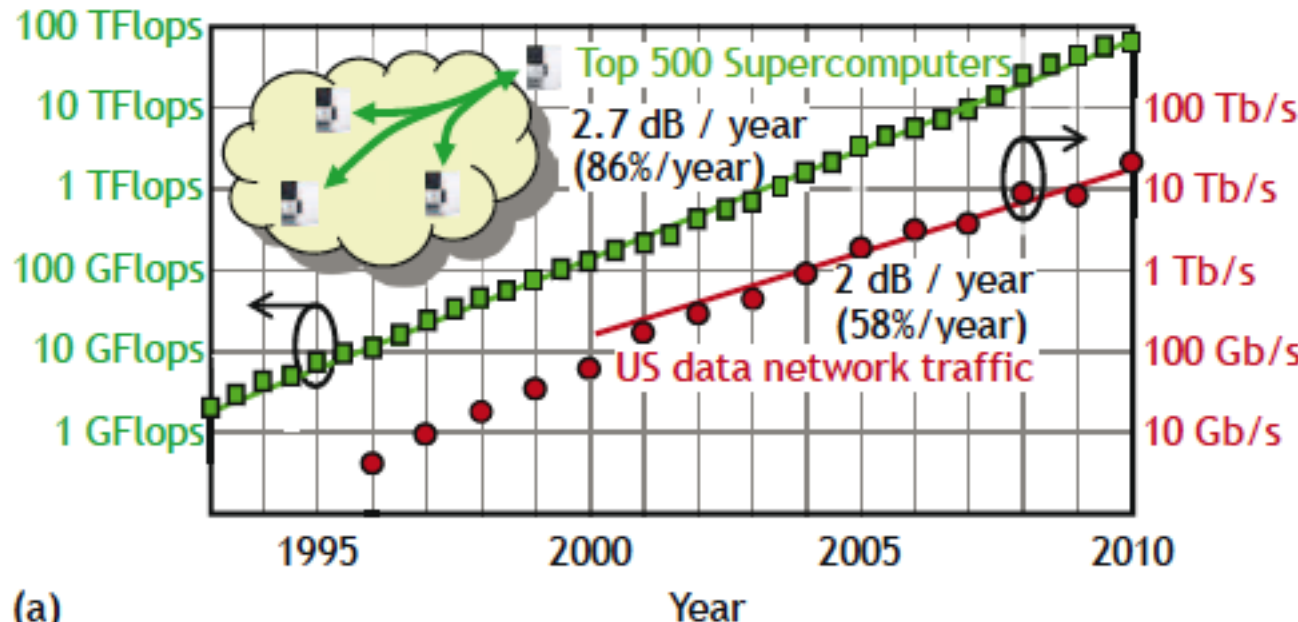
Spatial multiplexing in Telecommunications

MIMO capacities and outage probabilities in spatially multiplexed optical transport systems

Peter J. Winzer* and Gerard J. Foschini

Bell Labs, Alcatel-Lucent, 791 Holmdel-Keyport Rd., Holmdel, New Jersey 07733, USA

[*peter.winzer@alcatel-lucent.com](mailto:peter.winzer@alcatel-lucent.com)



(a)

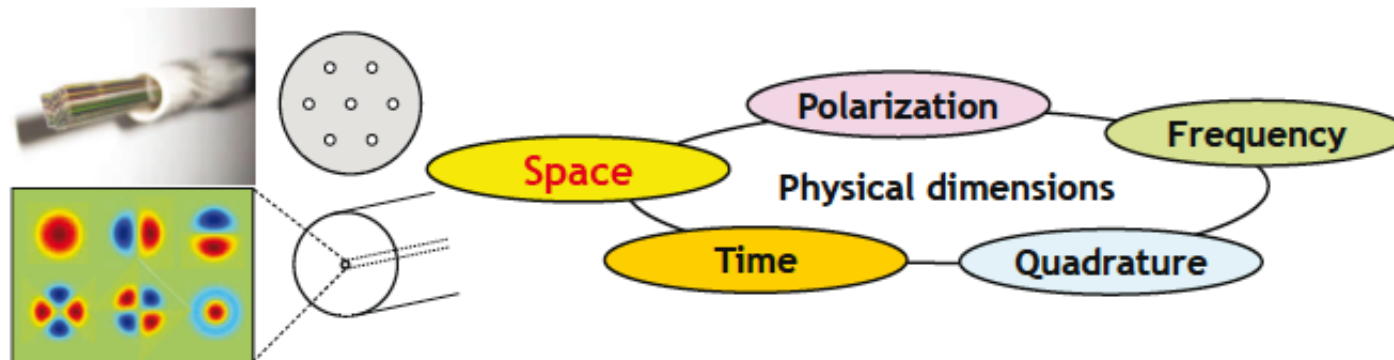
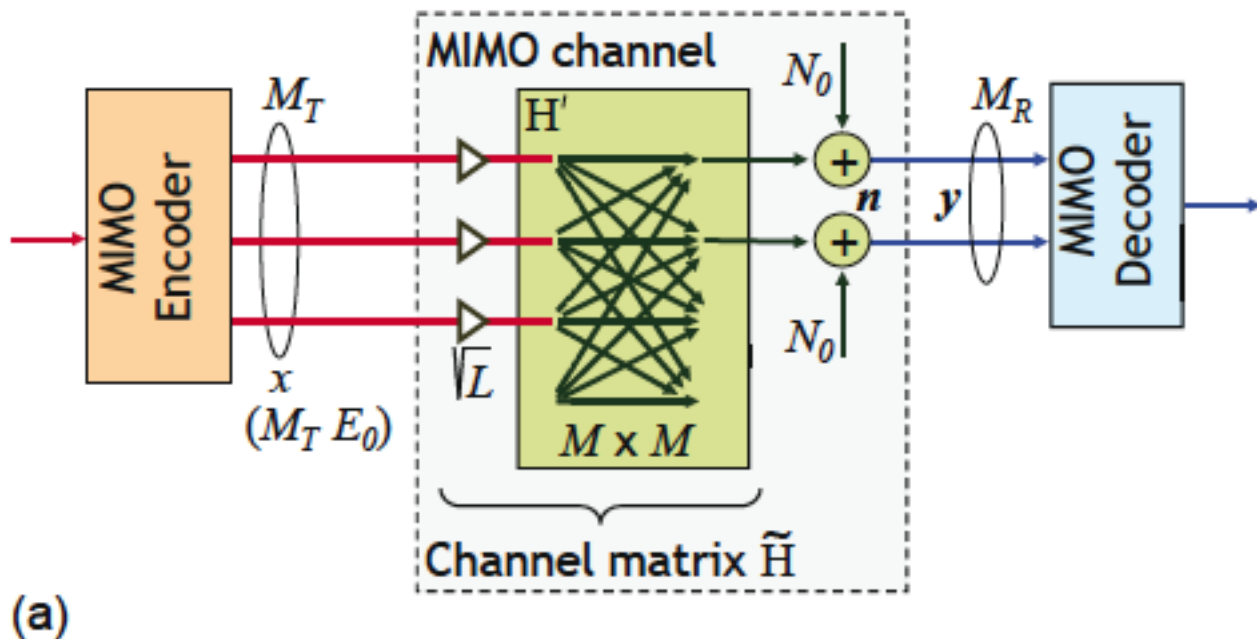


Fig. 2. Spatial multiplexing exploits the only known physical dimension that has not yet been used in optical transport systems. Implementations include fiber bundles, multi-core, and multi-mode fiber (Fig. after [10]).

The MIMO concept

Multiple (modes) In Multiple (modes) out

find the eigenstates of propagation



Coherent Optical MIMO (COMIMO)

Akhil R. Shah, Rick C. J. Hsu, Alireza Tarighat, *Student Member, IEEE*, Ali H. Sayed, *Fellow, IEEE*,
and Bahram Jalali, *Fellow, IEEE*

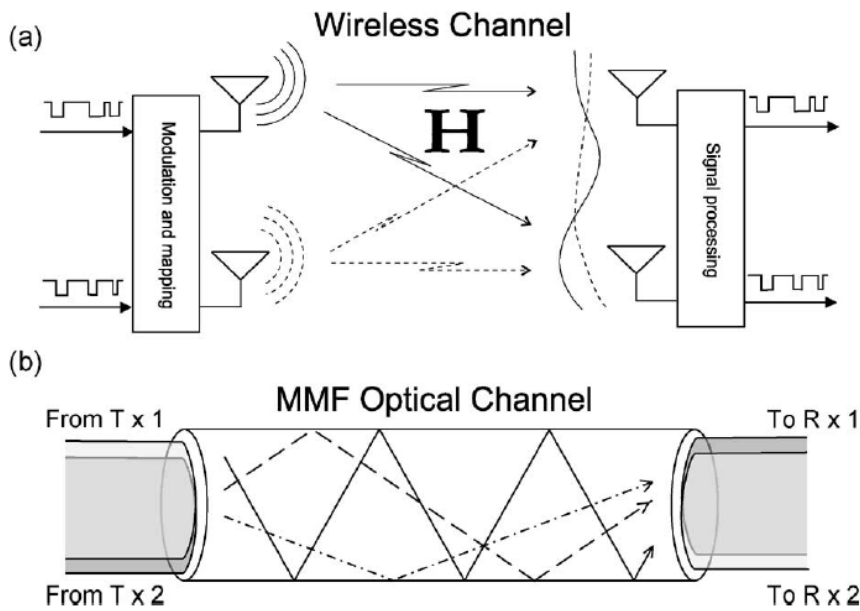


Fig. 1. (a) Coupling diversity into and out of MMF. (b) Ray tracing conceptual description of light beam scattering inside a multimode fiber.

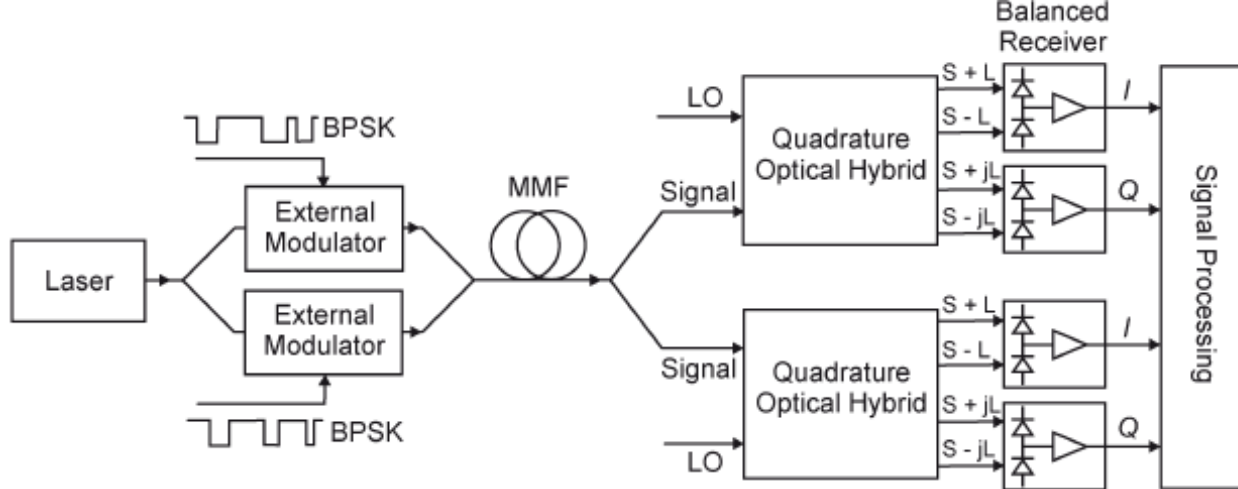
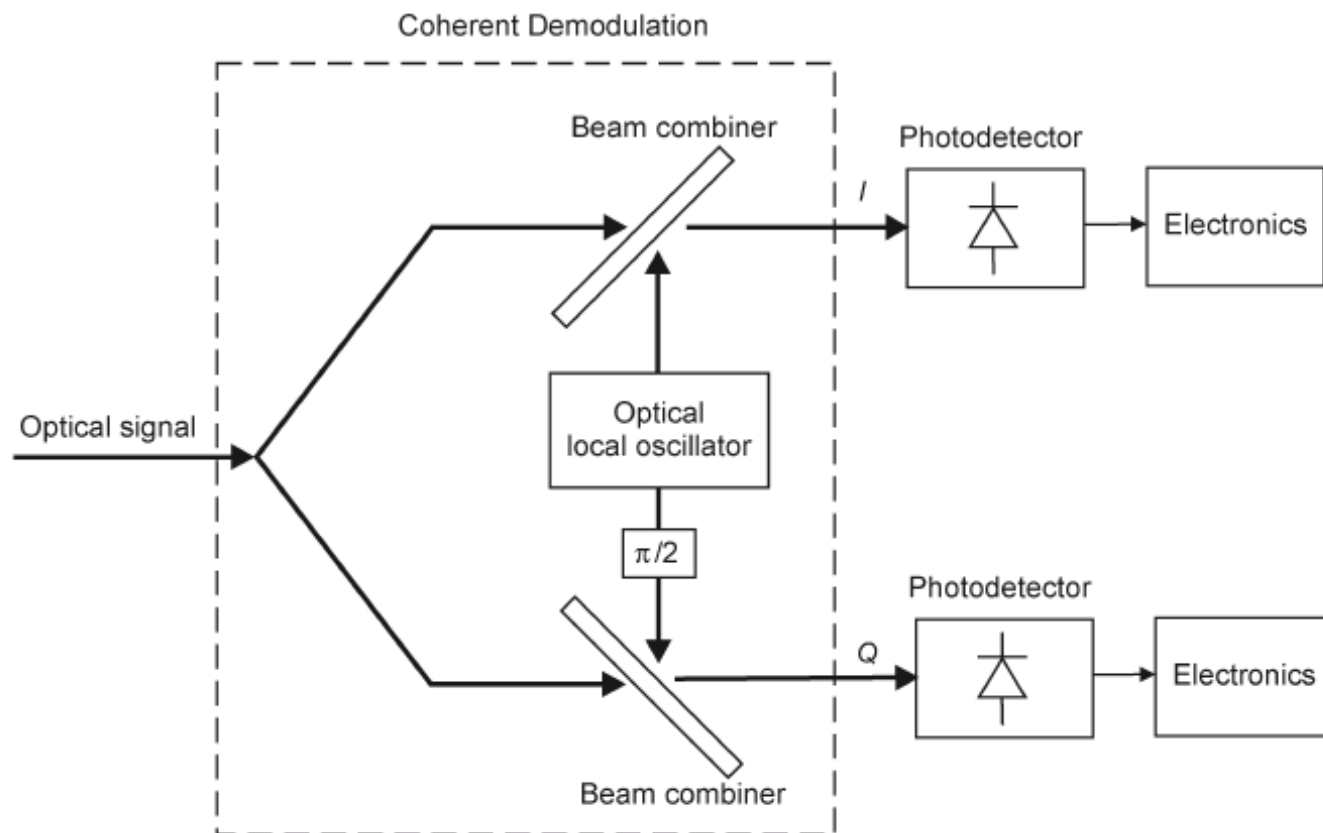


Fig. 2. Block diagram of COMIMO showing two independently modulated carriers and two receivers. Coupling diversity is not shown for simplicity.



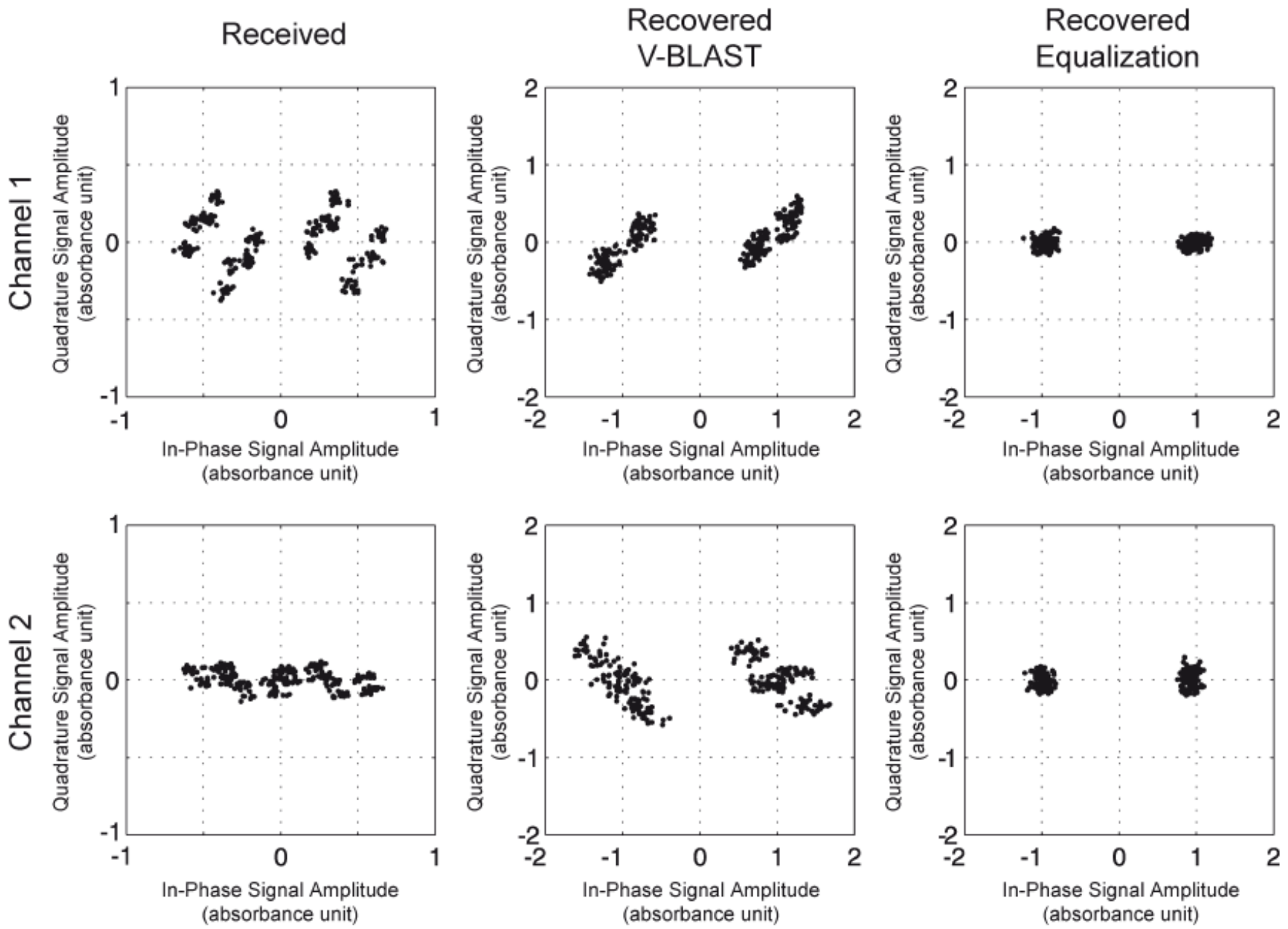
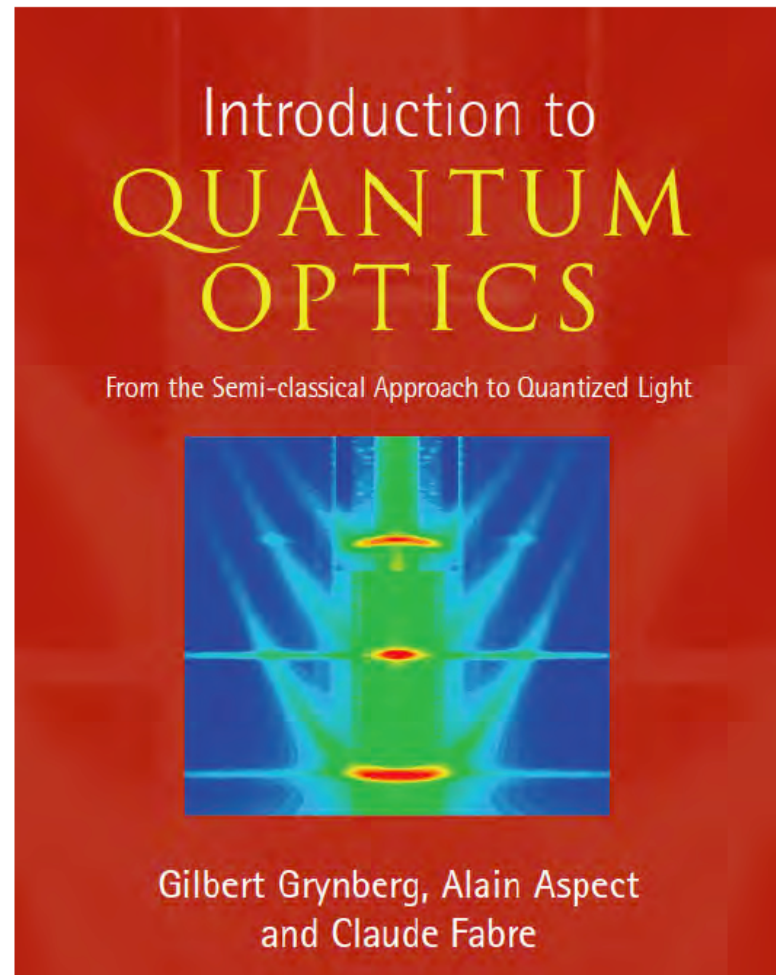


Fig. 5. Constellation diagrams showing received data from a wide-band channel (with ISI) and symbol recovery without equalization and with equalization.

FIELD QUANTIZATION



quantification requires modes

$$\hat{\mathbf{E}}^+(\mathbf{r}, t) = \sum_m E_0 \hat{a}_m \mathbf{f}_m(\mathbf{r}, t)$$

comes from quantization procedure:
linearity of quantum mechanics

comes from electromagnetism
linearity of Maxwell equations

most general quantum state of field

$$|\Psi\rangle = \sum_{n_1=0}^{\infty} \dots \sum_{n_m=0}^{\infty} \dots C_{n_1, \dots, n_m, \dots} |n_1 \text{ photons en } \mathbf{f}_1, \dots, n_m \text{ photons en } \mathbf{f}_m, \dots\rangle$$

double basis:

- of modes,
 - of states inside each mode
- both can be changed

Experimental characterization
of the temporal shape of the
principal modes or "supermodes"

Experimentally Accessing the Optimal Temporal Mode of Traveling Quantum Light States

Olivier Morin, Claude Fabre, and Julien Laurat*

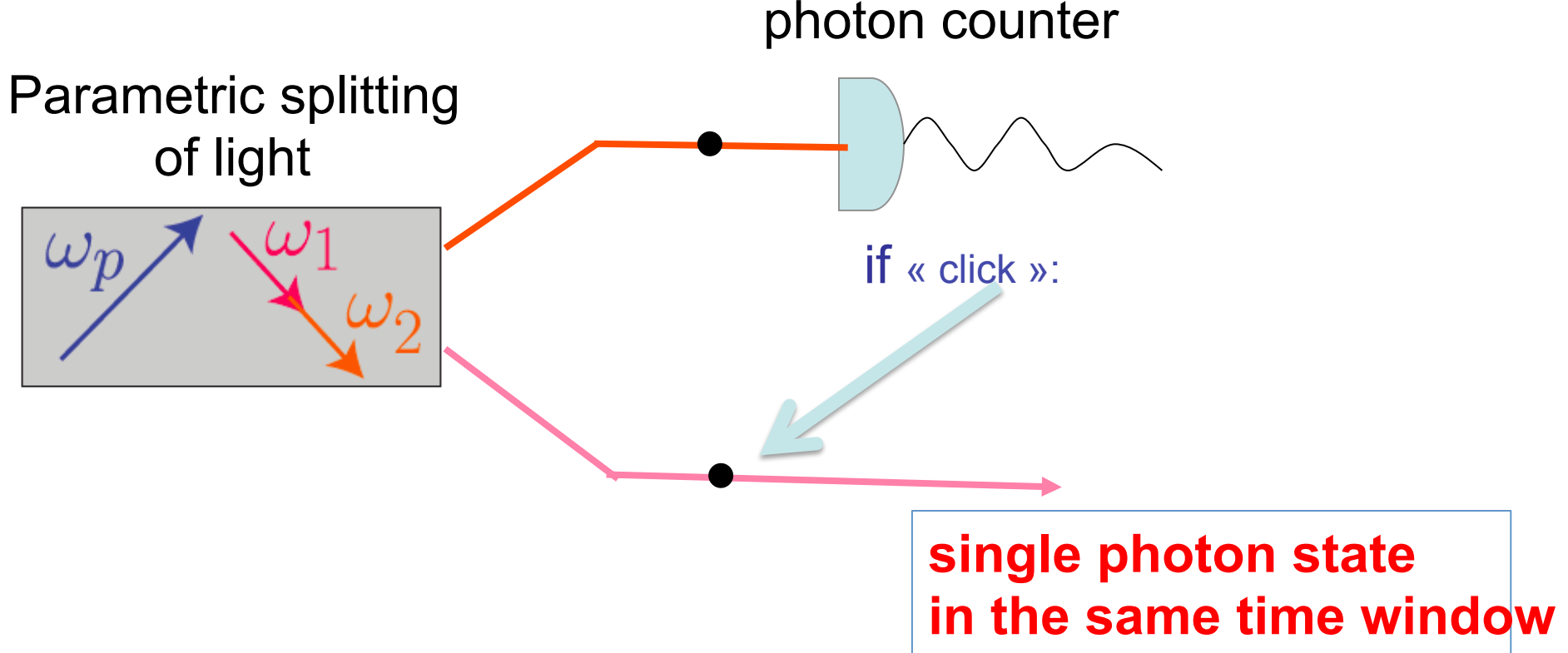
*Laboratoire Kastler Brossel, Université Pierre et Marie Curie, Ecole Normale Supérieure,
CNRS, 4 Place Jussieu, 75252 Paris Cedex 05, France*
(Received 14 June 2013; published 19 November 2013)

The characterization or subsequent use of a propagating optical quantum state requires the knowledge of its precise temporal mode. Defining this mode structure very often relies on a detailed *a priori* knowledge of the used resources, when available, and can additionally call for an involved theoretical modeling. In contrast, here we report on a practical method enabling us to infer the optimal temporal mode directly from experimental data acquired via homodyne detection, without any assumptions on the state. The approach is based on a multimode analysis using eigenfunction expansion of the autocorrelation function. This capability is illustrated by experimental data from the preparation of Fock states and coherent state superposition.

DOI: [10.1103/PhysRevLett.111.213602](https://doi.org/10.1103/PhysRevLett.111.213602)

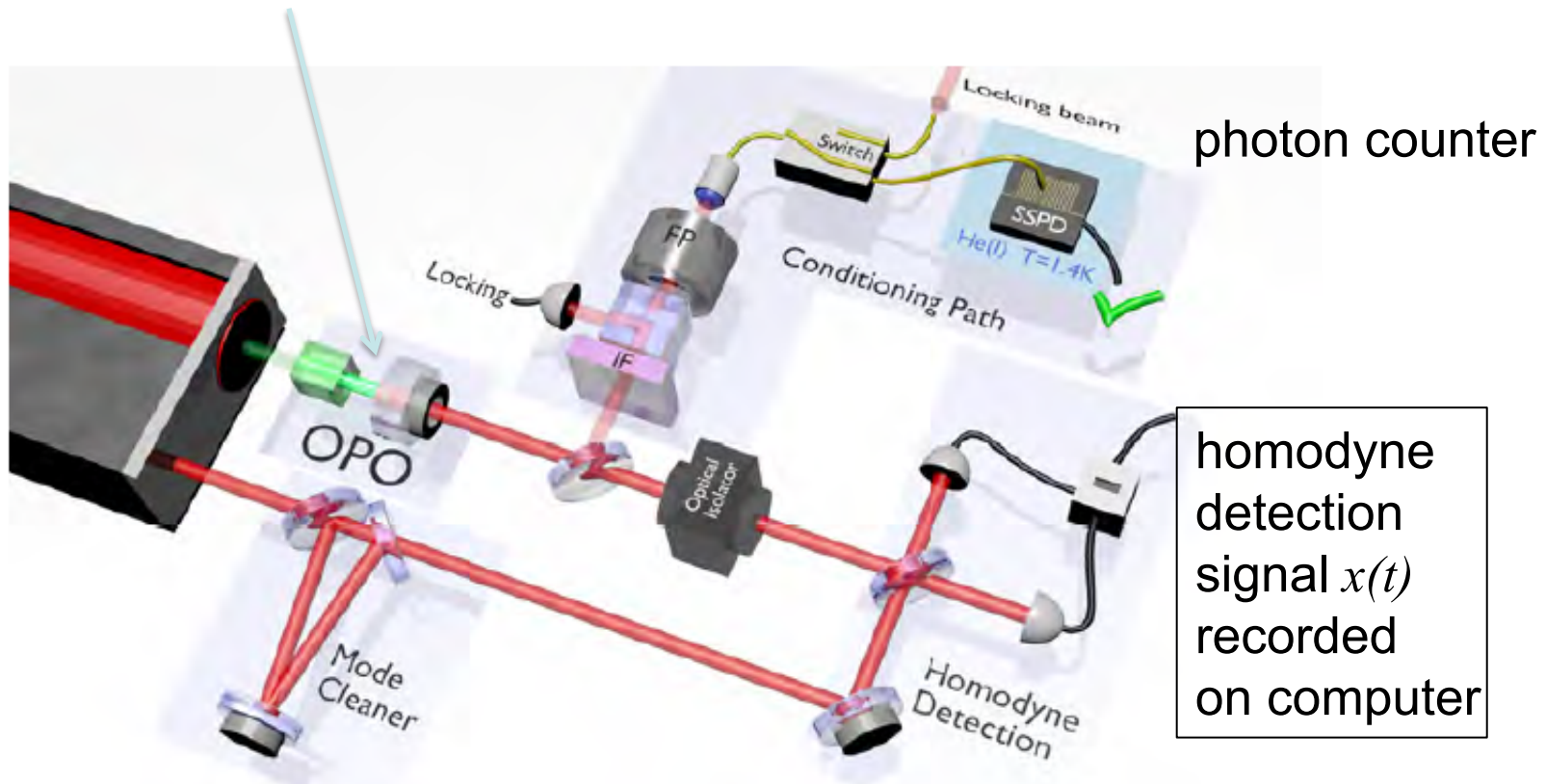
PACS numbers: 42.50.Dv, 03.65.Wj, 03.67.-a

conditional generation of single photons "heralded photons"



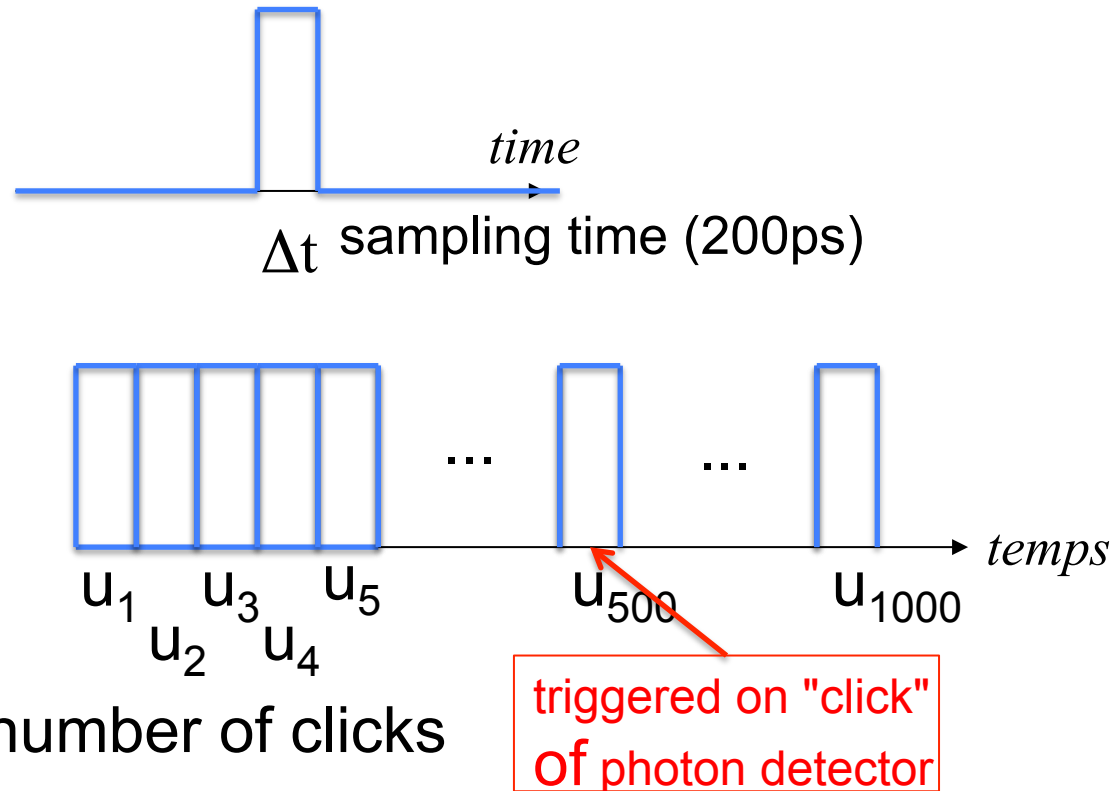
experimental set-up

Parametric crystal
inside an optical cavity



used modes : time bins

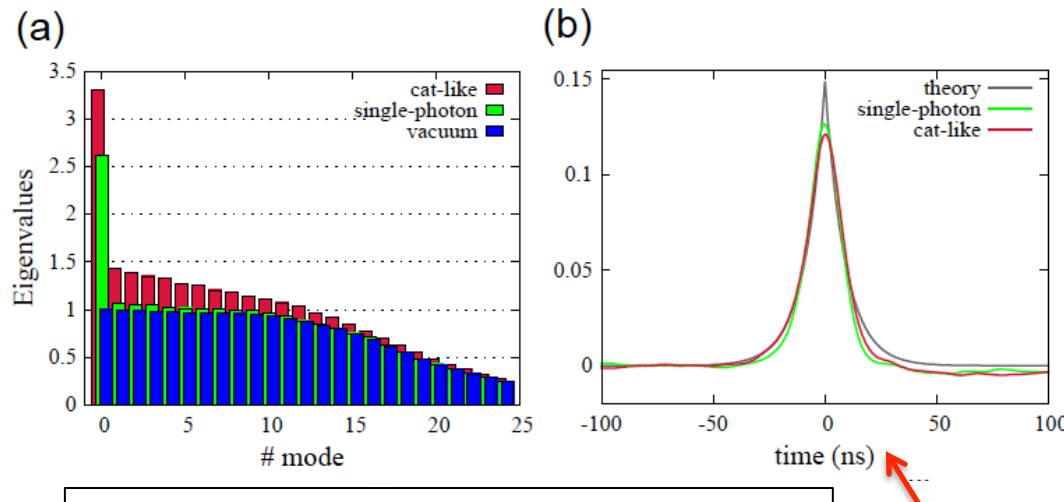
measured quantity :
 homodyne signal
 intensity during Δt
 (on a given quadrature)



averaged over a great number of clicks

$$\begin{bmatrix} \Delta^2 E_{X1} & C(E_{X1}E_{X2}) & \dots & C(E_{X1}E_{XN}) \\ C(E_{X2}E_{X1}) & \Delta^2 E_{X2} & \dots & C(E_{X2}E_{XN}) \\ \dots & \dots & \dots & \dots \\ C(E_{XN}E_{X1}) & C(E_{XN}E_{X2}) & \dots & \Delta^2 E_{XN} \end{bmatrix}$$

1000× 1000 covariance matrix of a single quadrature, which can be diagonal



eigen values of covariance matrix

1: level of vacuum fluctuations ($=E_0^2$)

only one eigen value different from vacuum fluctuations
the generated state is single mode

time shape of temporal mode

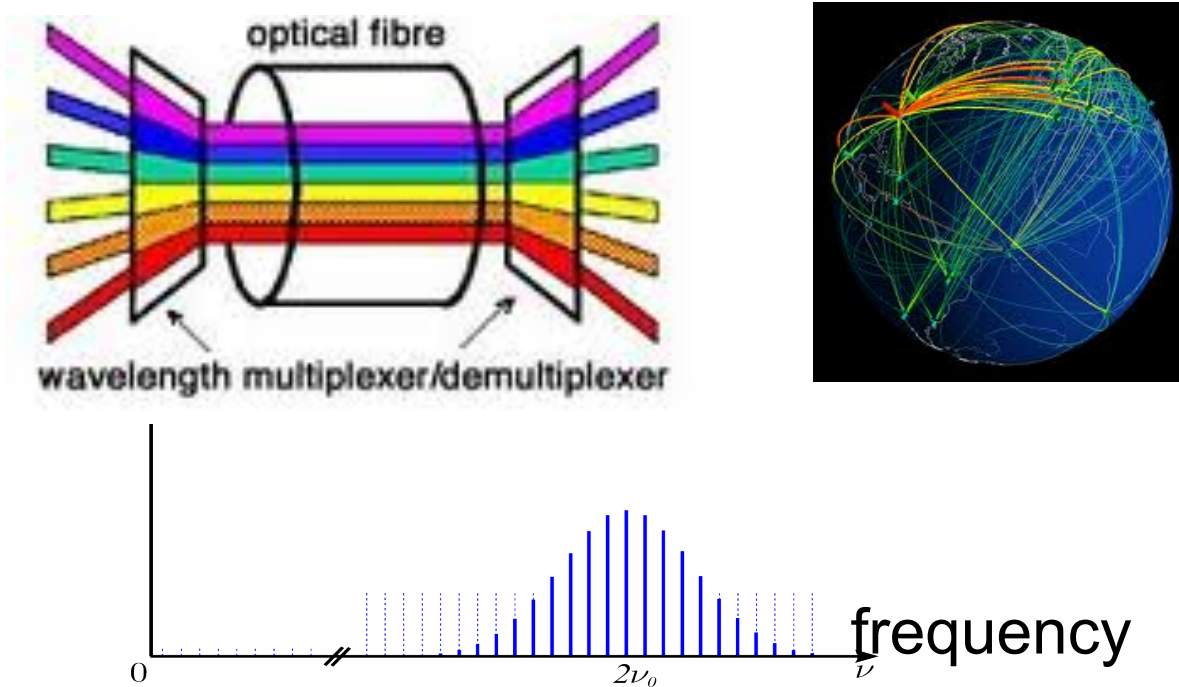
it corresponds to the temporal mode of the OPO cavity
 (=Fourier transform of cavity spectrum)

$$e^{-|t-t_{trigger}|/T_{cav}}$$

*manipulation
of frequency modes*

"quantum frequency combs"

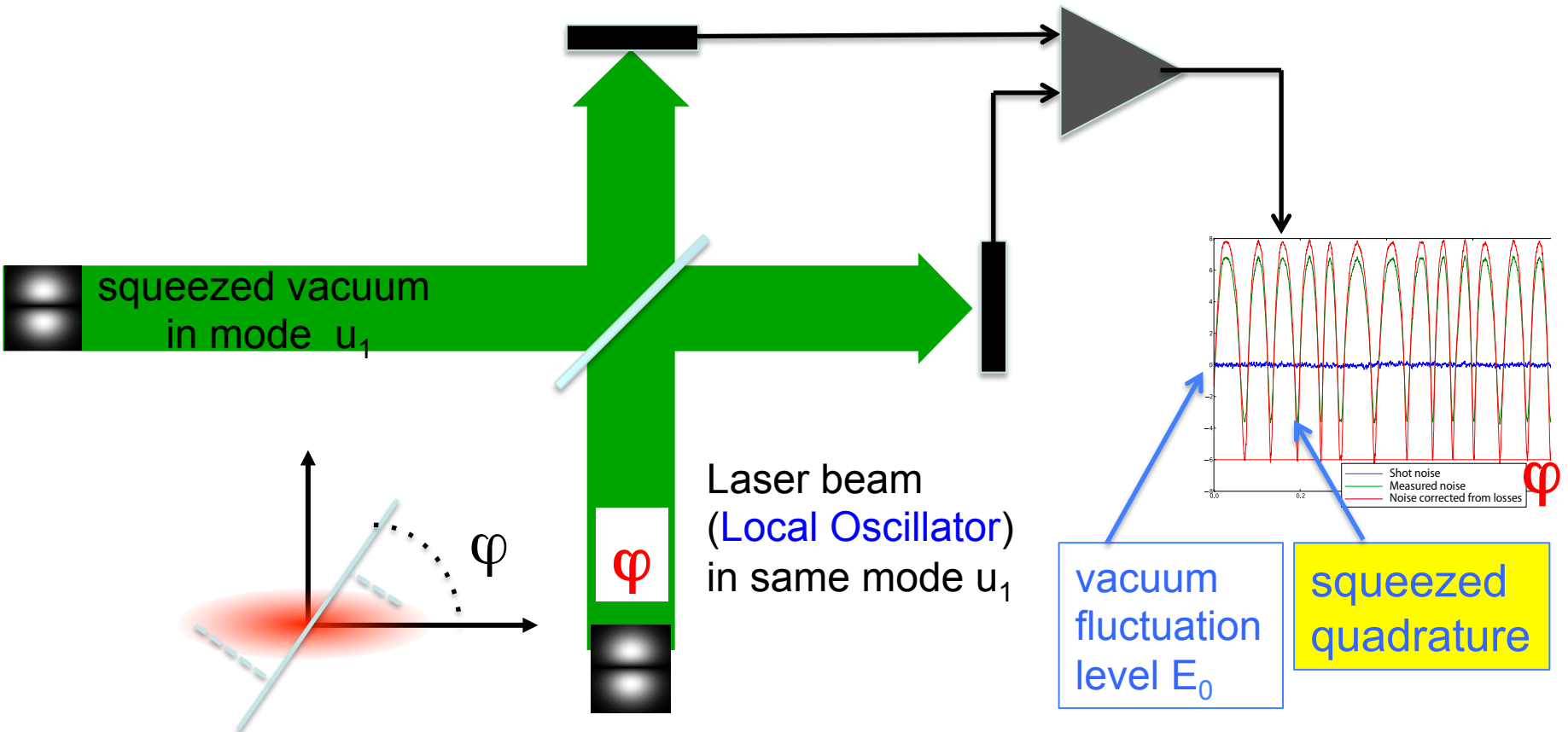
The quantum analogue of Wavelength Division Multiplexing (WDM) ?



multi-frequency quantum state

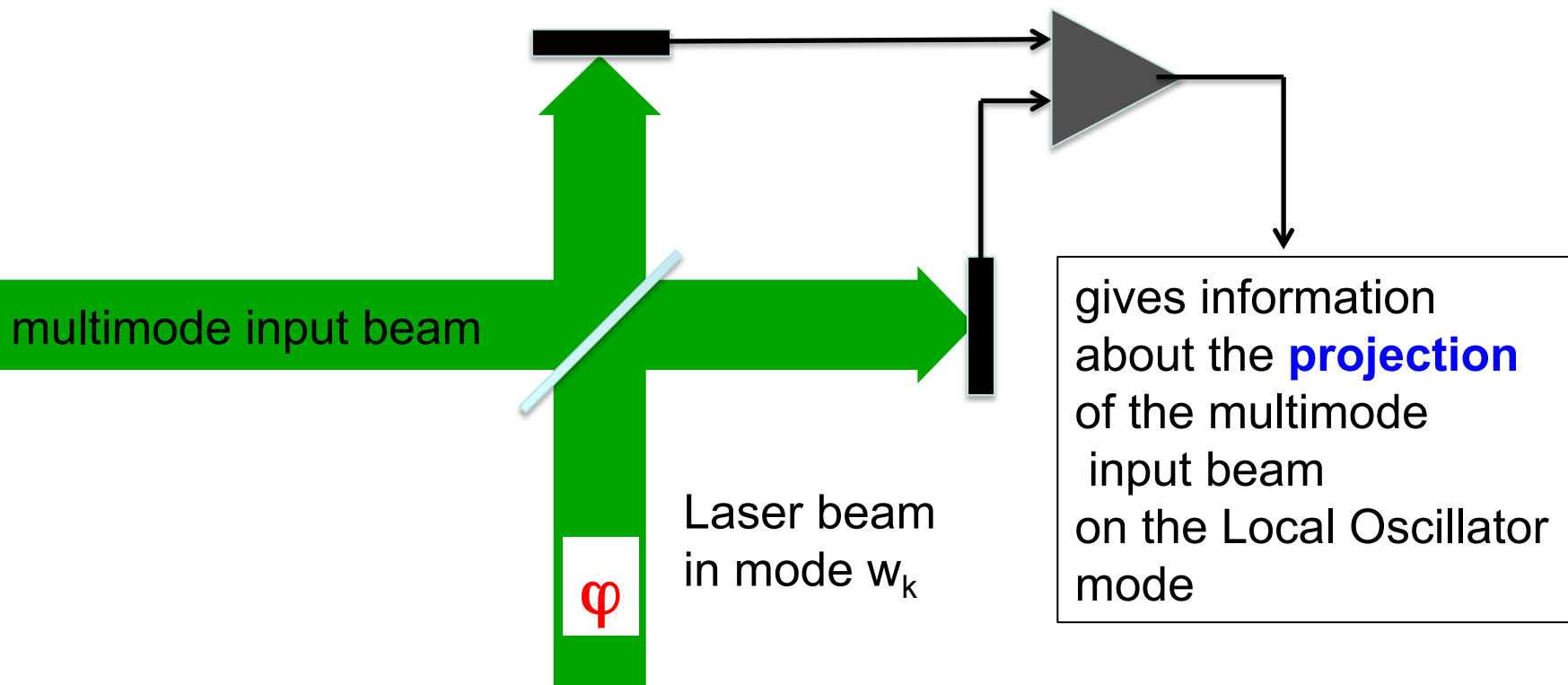
many modes easily accessible :
a way to massively parallel quantum information processing ?

Balanced homodyne detection of squeezed vacuum



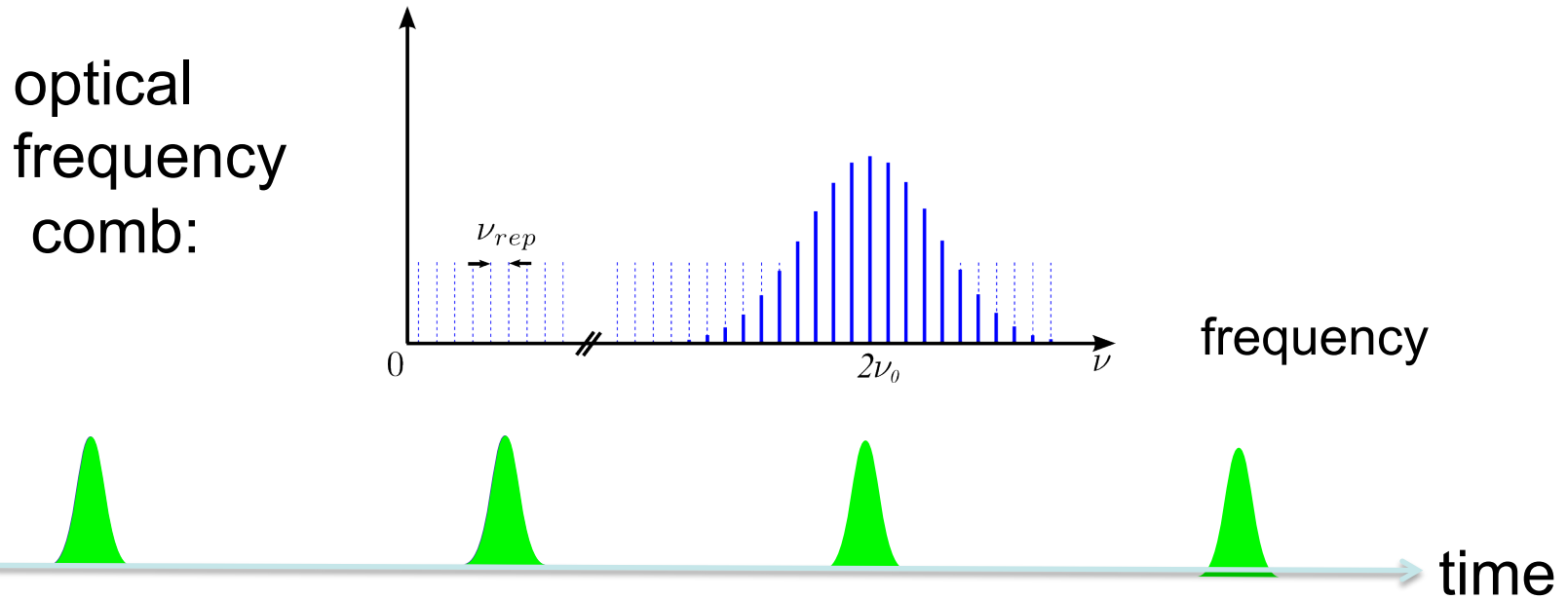
How to analyze the modal content of a multimode light state ?

- use several homodyne detections



one performs a series of homodyne measurements on **a set of modes** $\{w_k(\mathbf{r}, t)\}$

The frequency comb

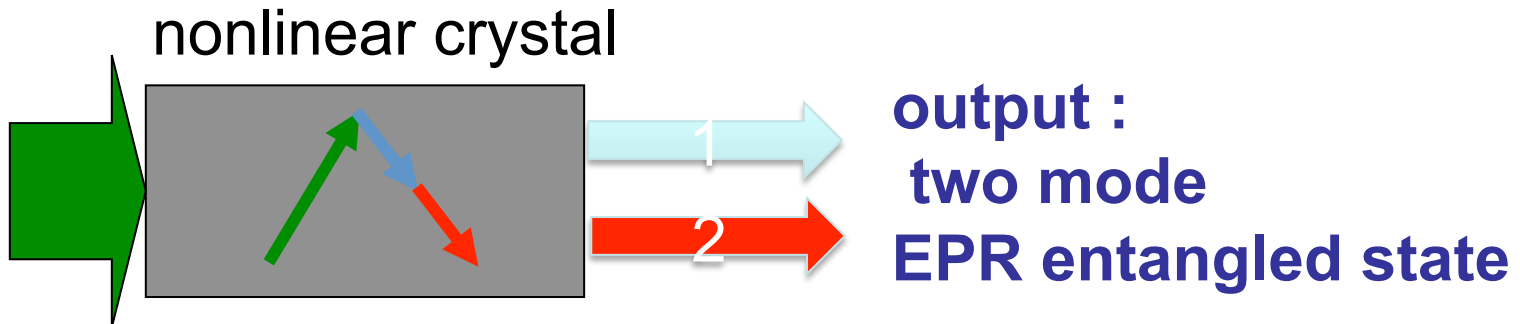


Frequency modes of a mode-locked laser: **about 100.000**

Can we entangle all these modes ?

Can we perform quantum computing operations
on all these modes ?

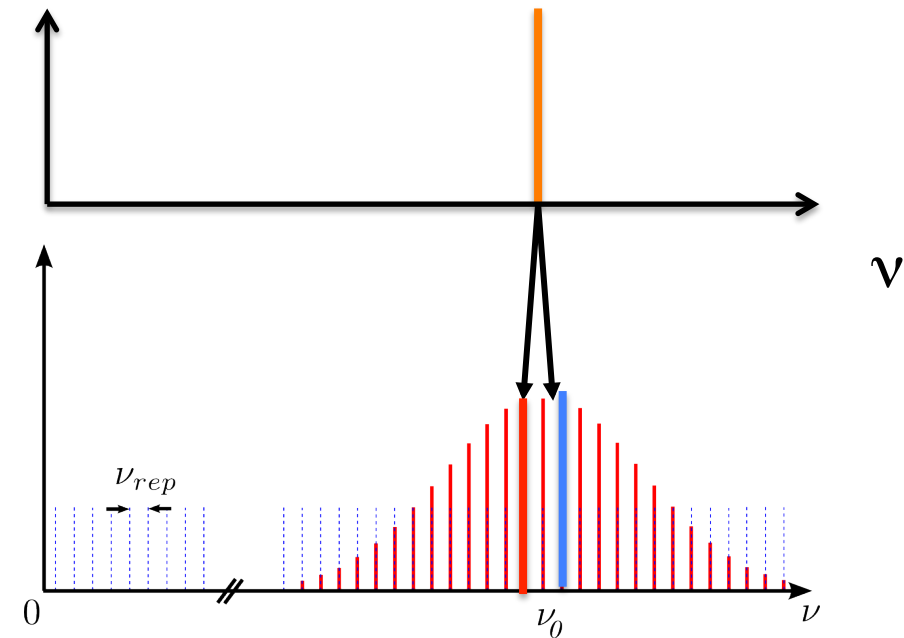
Parametric down conversion of monochromatic pump



- for a monochromatic pump

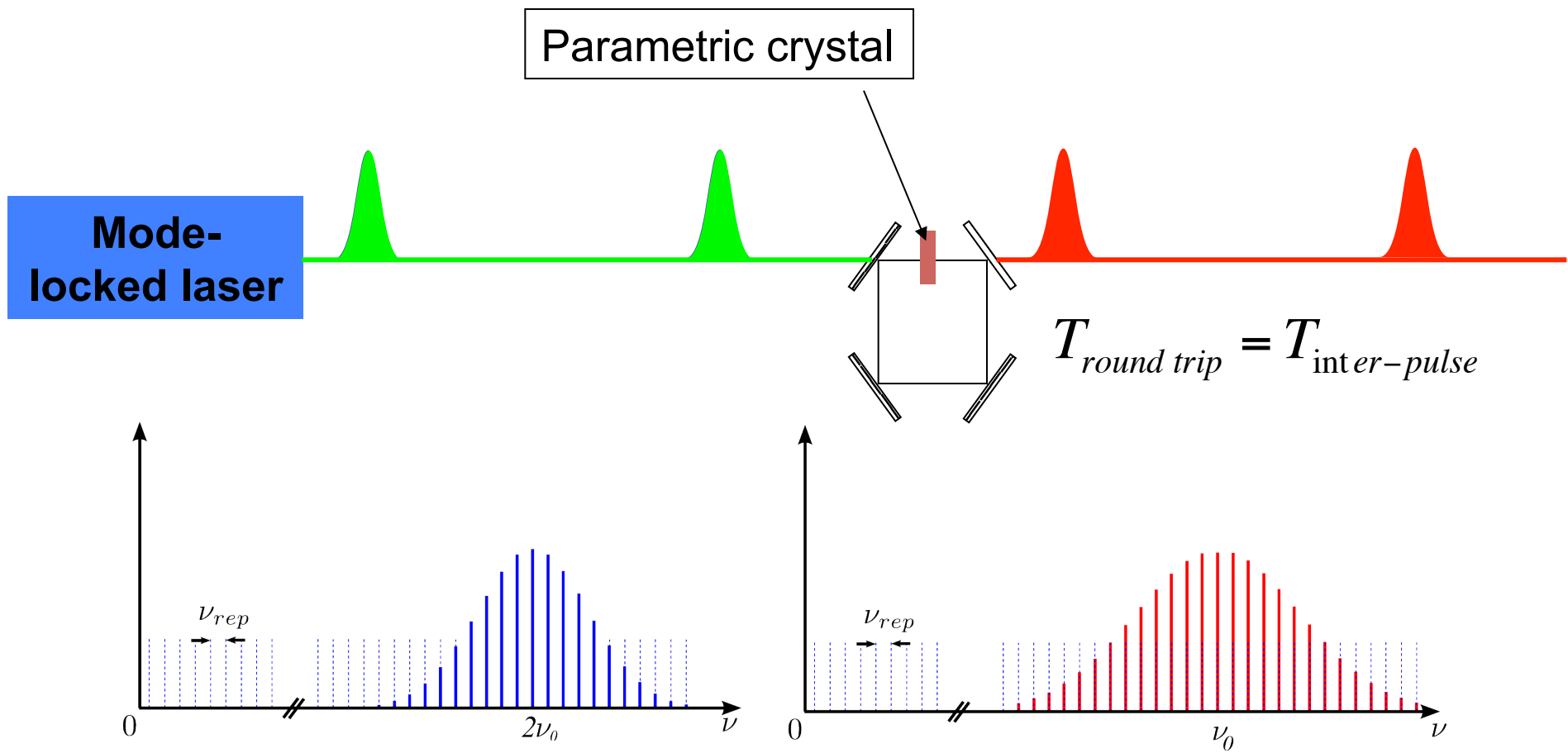
spectrum of down-converted light:

$$\nu_{signal} + \nu_{idler} = \nu_{pump}$$

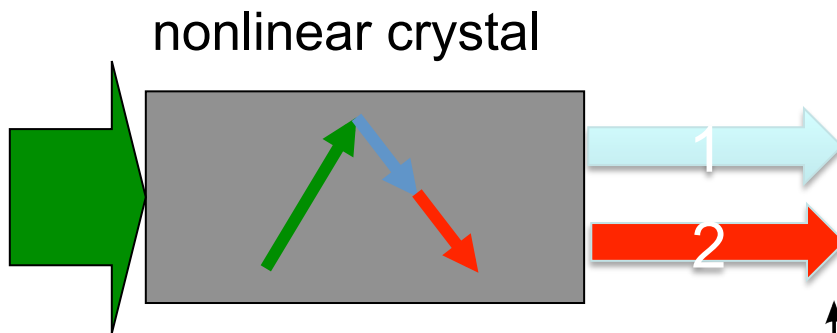


- creates independent couples of EPR entangled modes

the Synchronously Pumped Optical Parametric Oscillator (SPOPO)



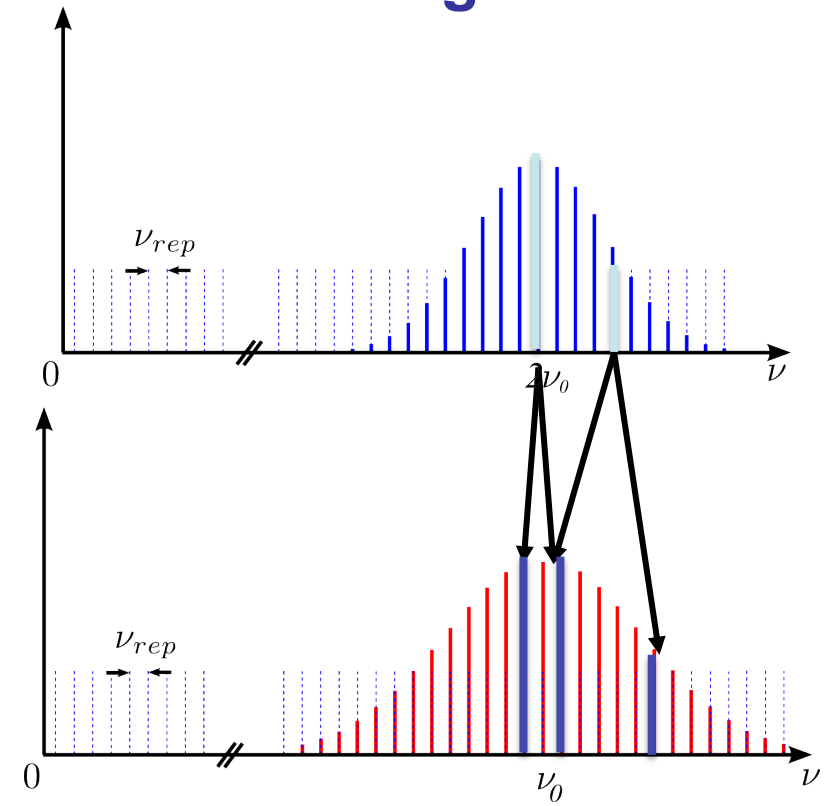
Parametric down conversion of a frequency comb



output :
two mode
EPR entangled state

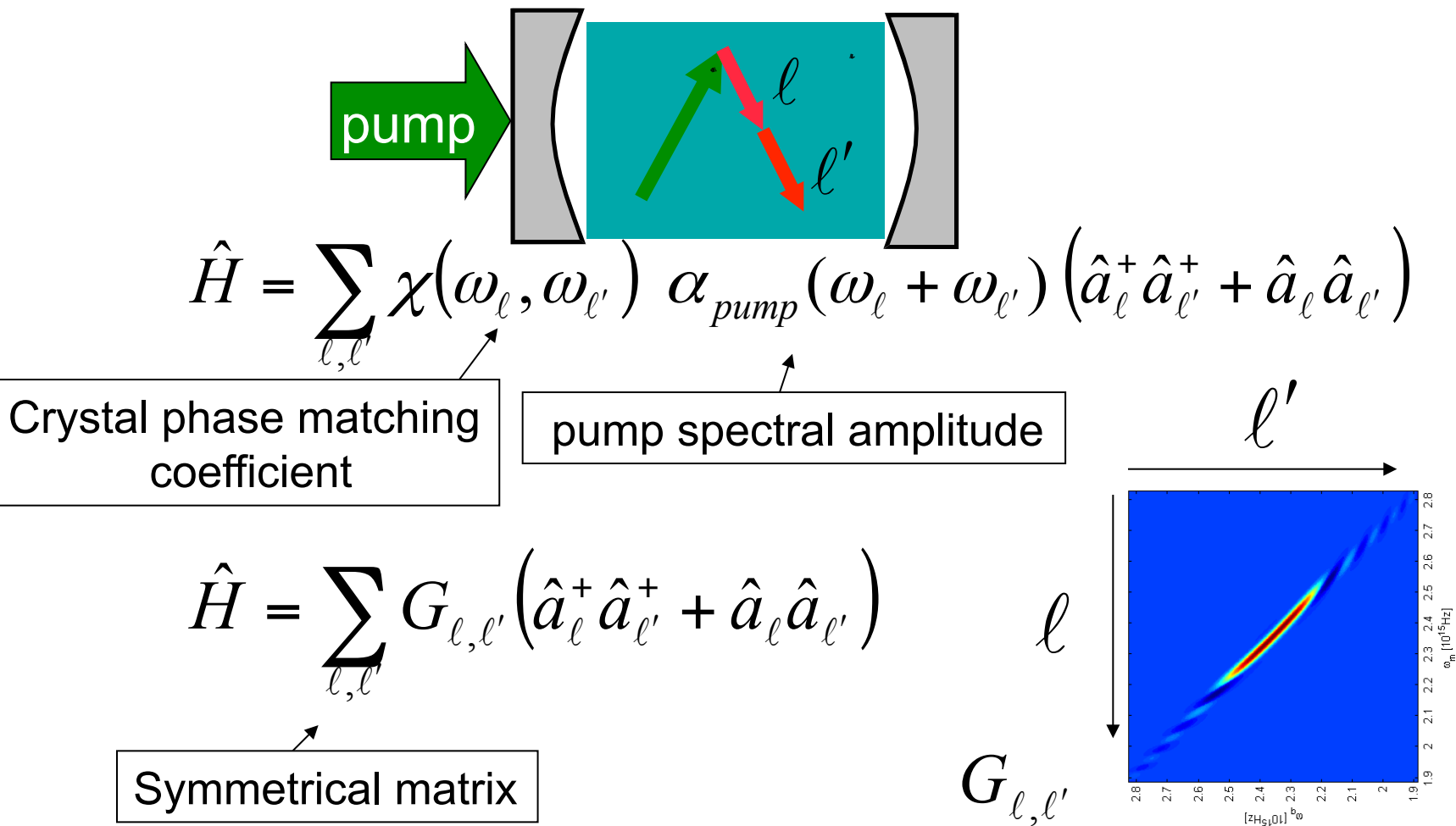
- for a frequency comb pump

spectrum of down-converted light:



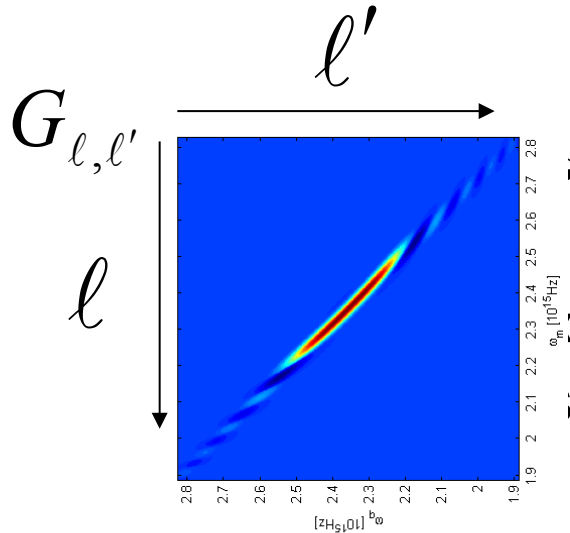
- all couples of frequencies should be entangled

A liitle bit of theory ...



G. De Valcarcel, G. Patera, N. Treps, C. Fabre, Phys. Rev. A**74**, 061801(R) (2006)
 Shifeng Jiang, N. Treps, C. Fabre, New Journal of Physics, **14** 043006 (2012)

Diagonalizing the interaction



► Eigenstates:
near combinations of frequency modes

"supermodes" $\hat{b}_k = \sum_{\ell} U_k^{\ell} \hat{a}_{\ell}$

eigenvalues Λ_k

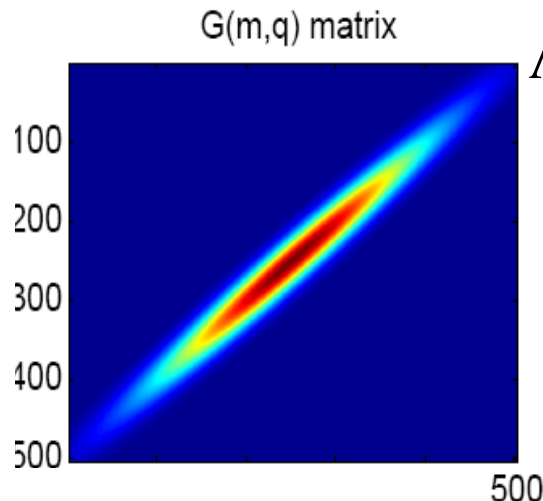
$$\hat{H} = \hbar \sum_{k=1}^{N_m} \Lambda_k \left(\hat{b}_k^2 + \hat{b}_k^{+2} \right)$$

:multi-squeezing hamiltonian

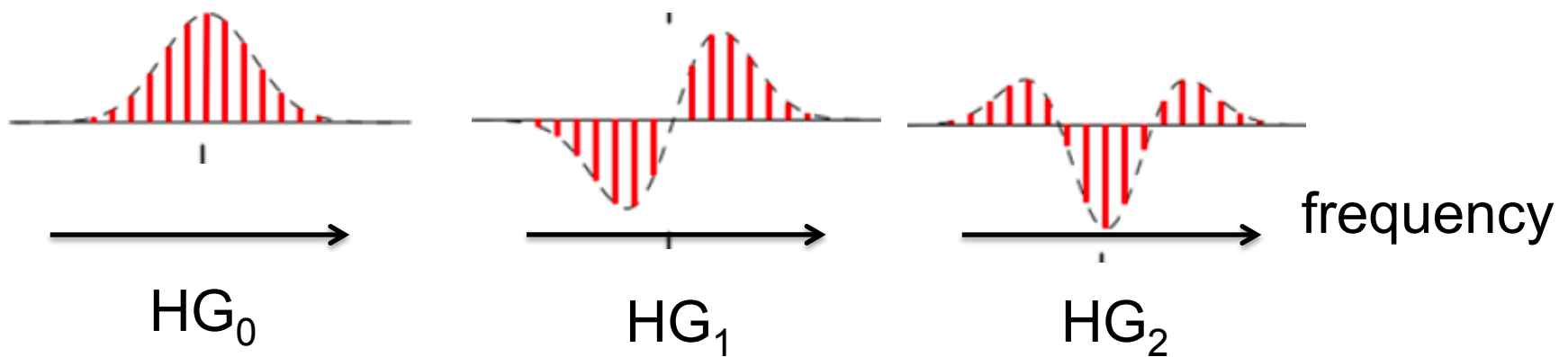
$$|\Psi_{\text{out}}\rangle = |\text{Squeezed state}_k(\Lambda_1)\rangle \otimes \dots \otimes |\text{Squeezed state}_k(\Lambda_{N_m})\rangle \otimes |0\rangle \otimes \dots$$

supermode shapes

Simple example: Gaussian variation of $G_{\ell,\ell'}$

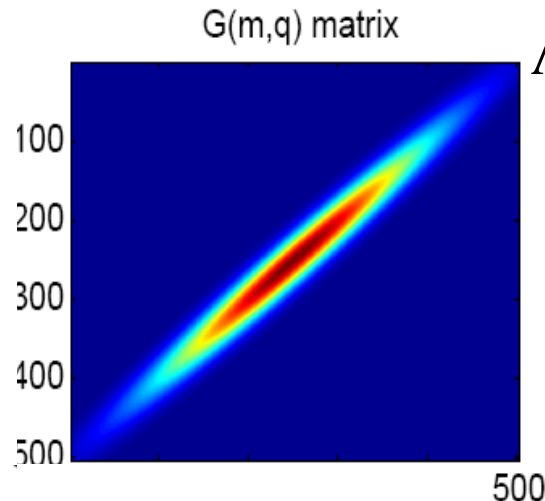


Eigenmodes: combs with Hermite-Gauss modal amplitudes

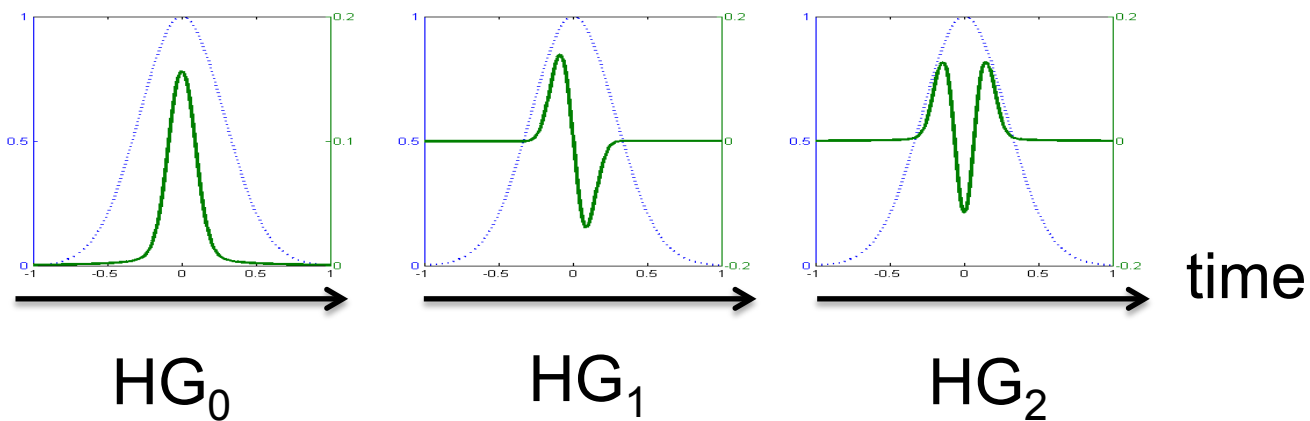


supermode shapes

Simple example: Gaussian variation of $G_{\ell,\ell'}$



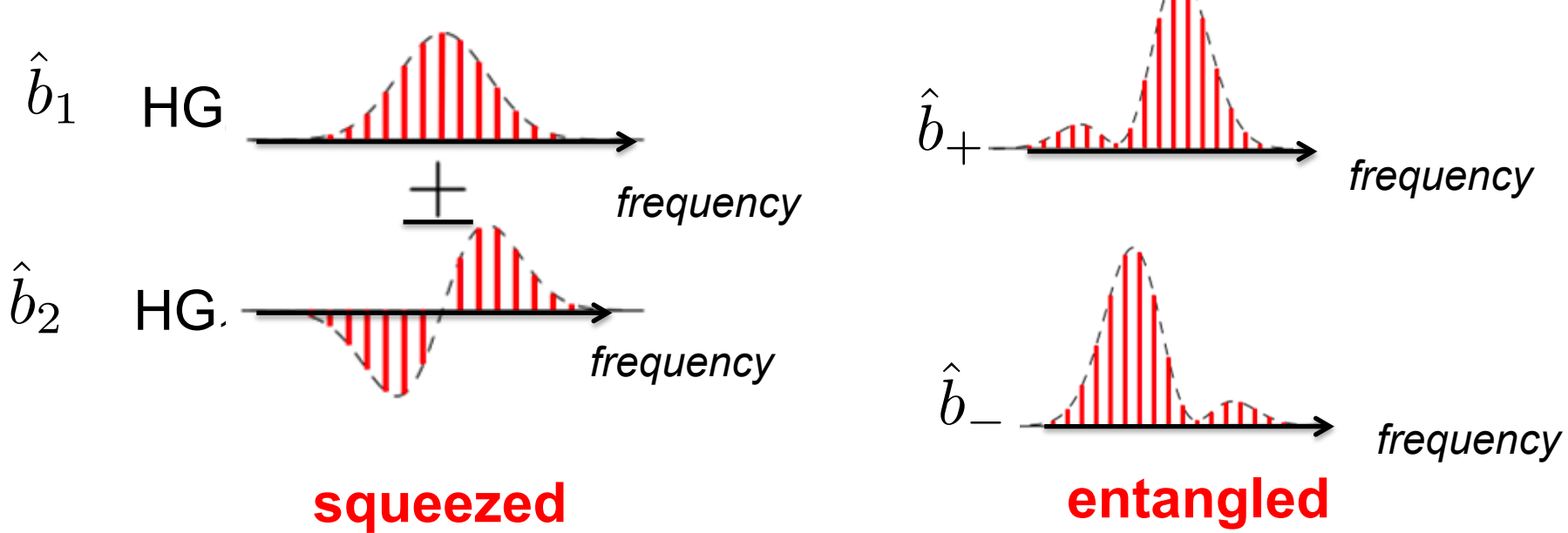
Eigenmodes: trains of pulses with Hermite-Gauss temporal shapes



entanglement: another choice of mode basis

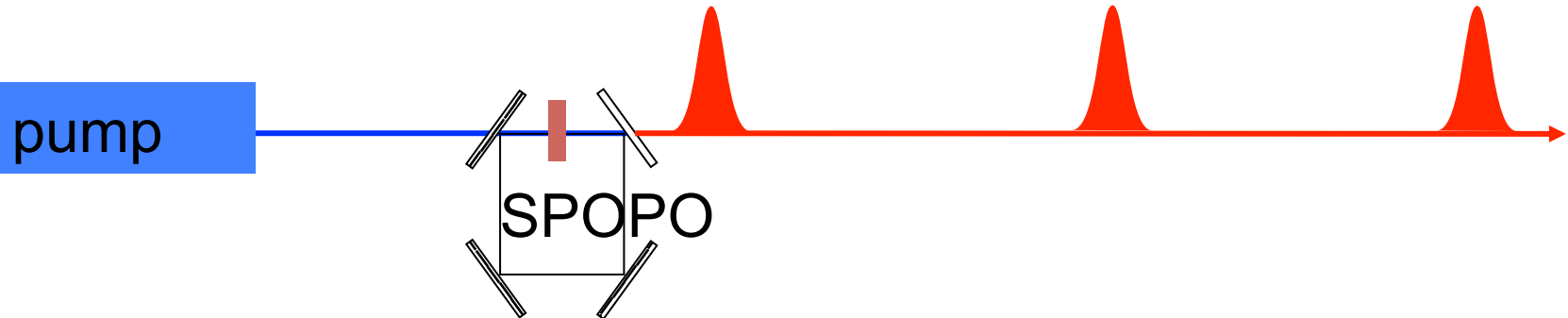
➤ Starting from two squeezed supermodes \hat{b}_1 \hat{b}_2

the mixed modes $\hat{b}_{\pm} = \frac{1}{\sqrt{2}}(\hat{b}_1 \pm \hat{b}_2)$
are EPR entangled

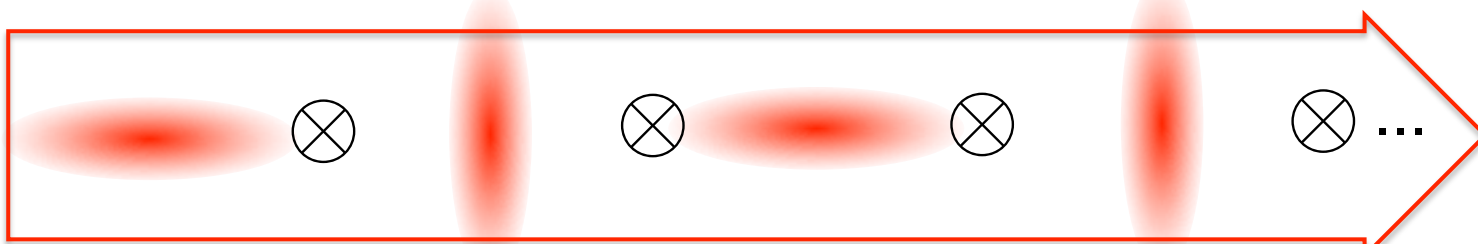


there will be entanglement
between different spectral parts of the comb

quantum state at SPOPO output



- factorized squeezed vacuum states in supermode basis



- multipartite entangled state in frequency mode basis



it depends on the way one looks at it !

Experiment

Wavelength-multiplexed quantum networks with ultrafast frequency combs

Jonathan Roslund, Renné Medeiros de Araújo, Shifeng Jiang, Claude Fabre and Nicolas Treps*

 Selected for a [Viewpoint](#) in *Physics*

PHYSICAL REVIEW A **89**, 053828 (2014)



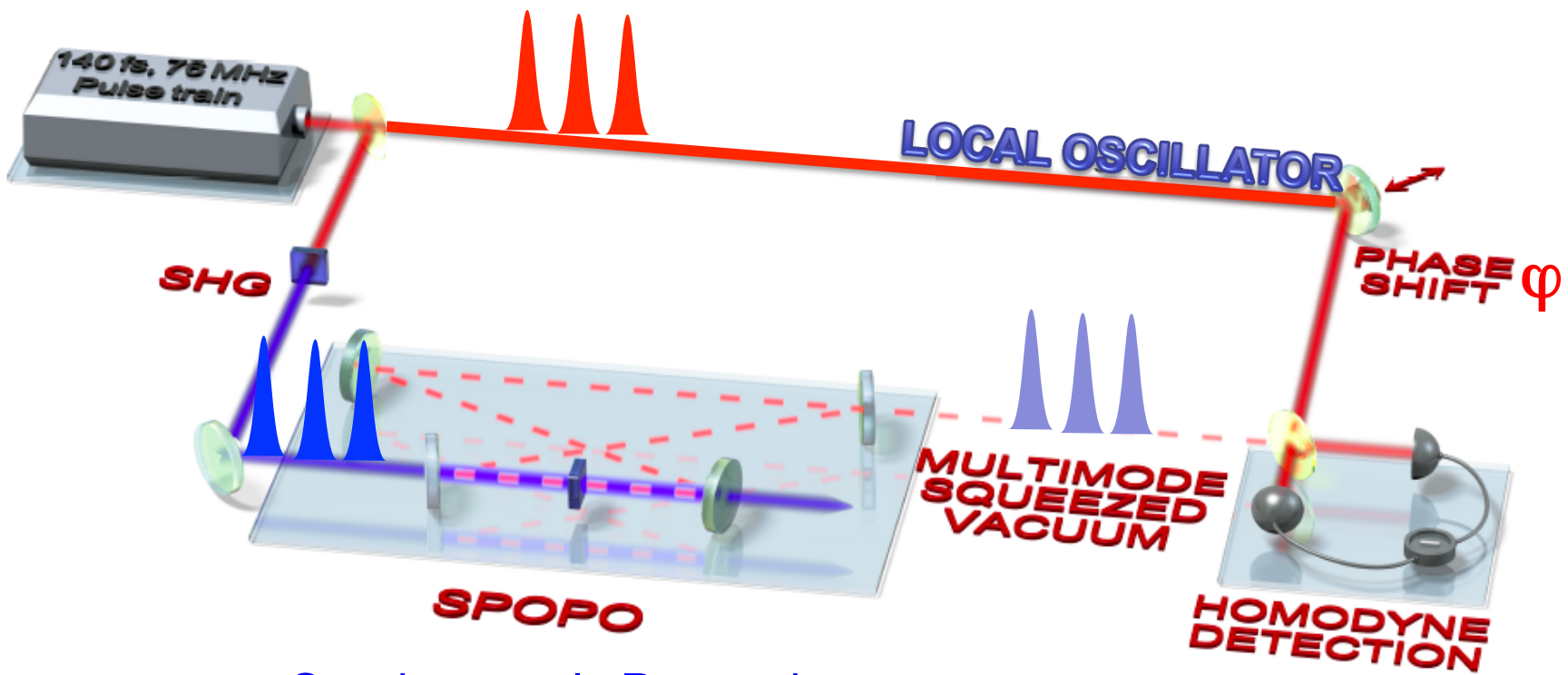
Full characterization of a highly multimode entangled state embedded in an optical frequency comb using pulse shaping

R. Medeiros de Araújo, J. Roslund, Y. Cai, G. Ferrini, C. Fabre, and N. Treps

Laboratoire Kastler Brossel, UPMC University of Paris 6, ENS, CNRS, 4 place Jussieu, 75252 Paris, France

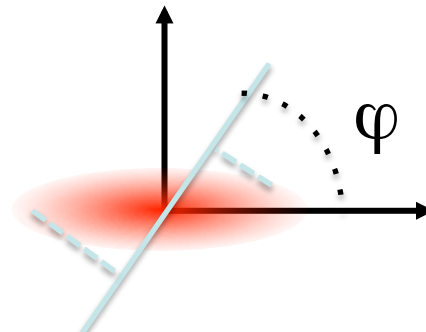
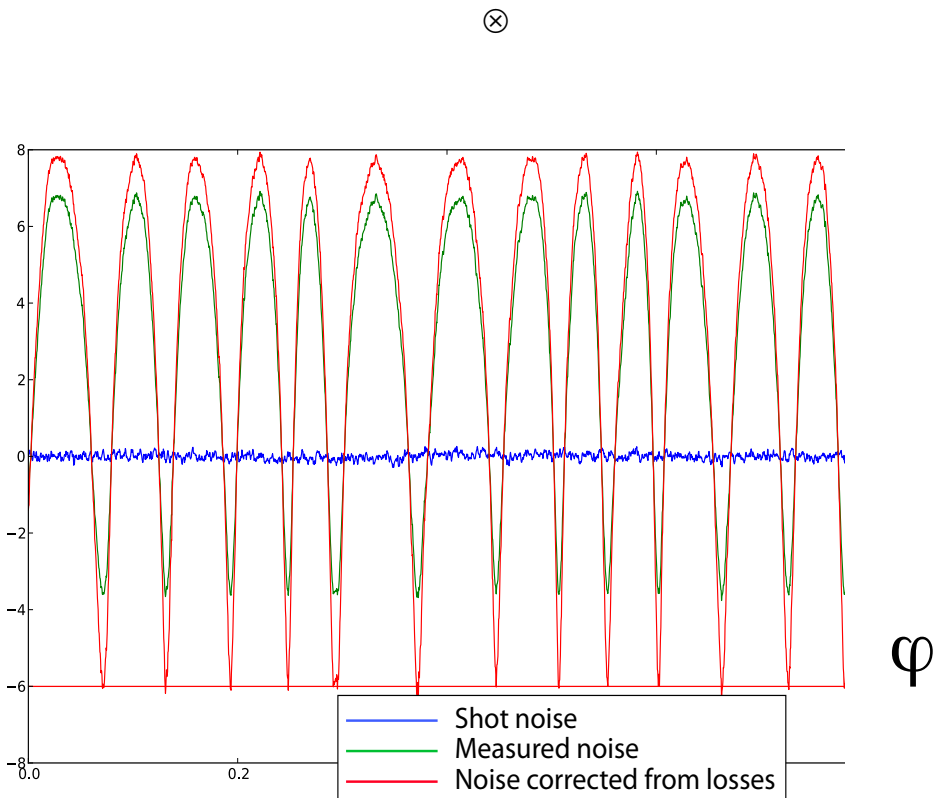
(Received 17 January 2014; published 27 May 2014)

Experimental set-up



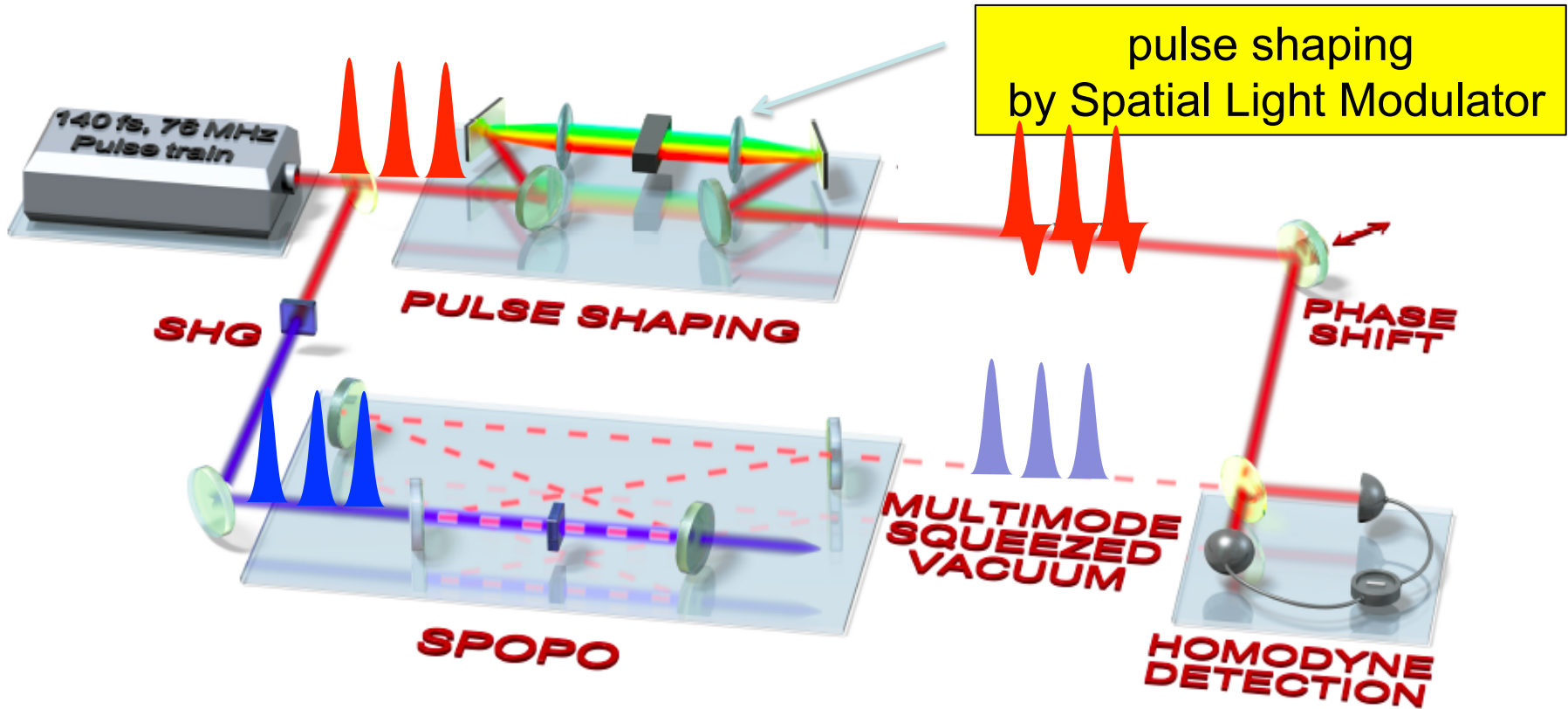
Synchronously Pumped
Optical Parametric Oscillator
operated below threshold

Homodyne detection measurement using pump laser as Local Oscillator

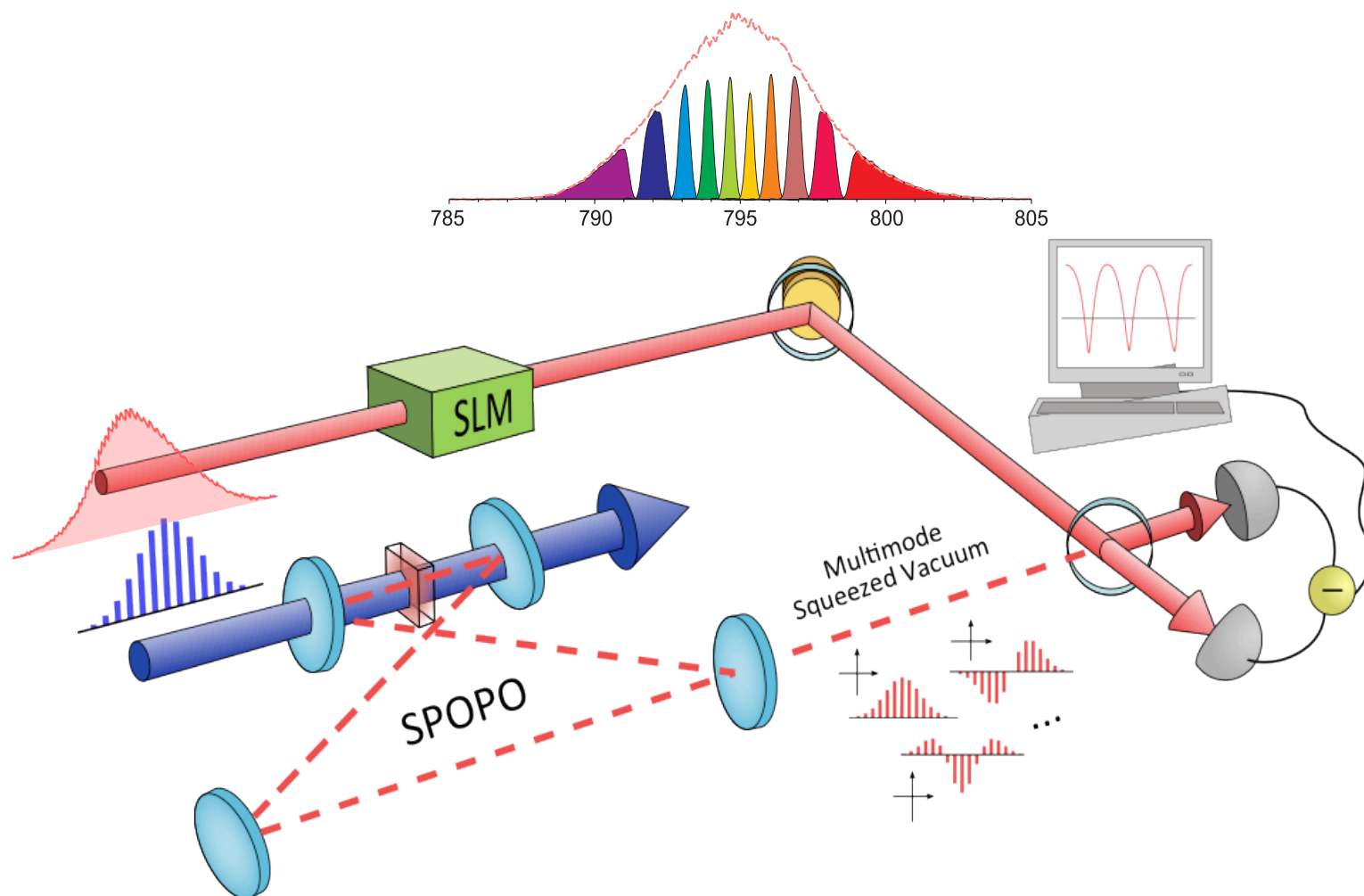


4dB (6 dB inferred) squeezed vacuum

characterization of multimode frequency comb: multiple homodyne detection with pulse-shaped LO



(1) : mode analysis in frequency space : multiple frequency bands (6 to 10)

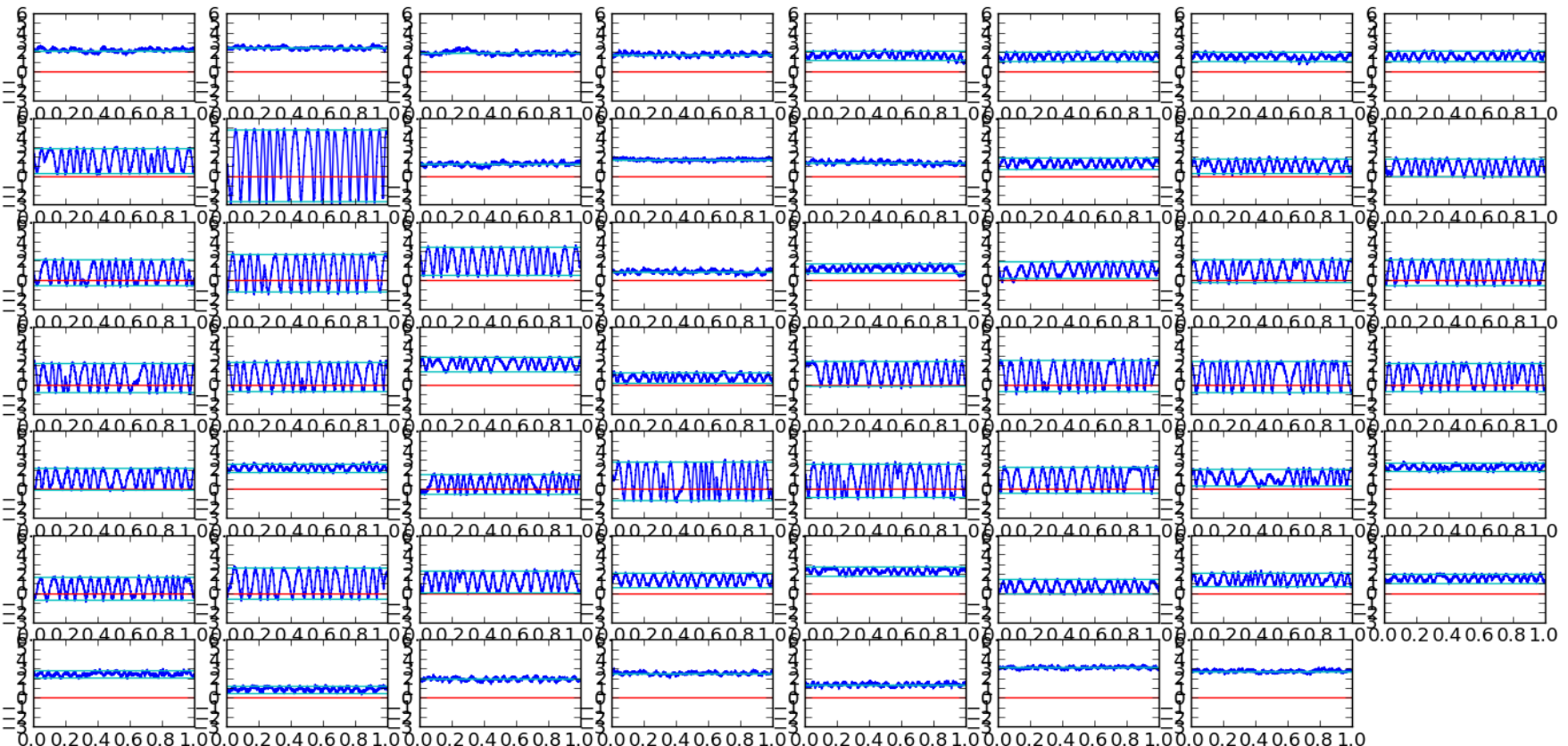


complete determination of the noise covariance matrix

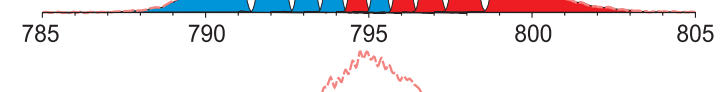
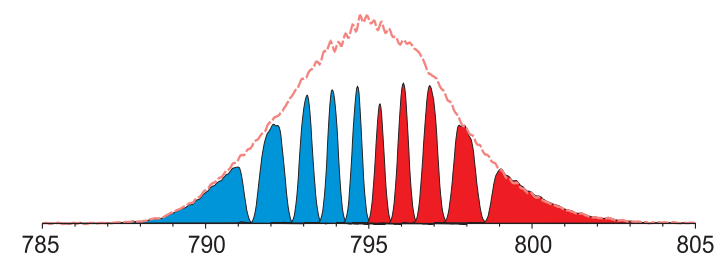
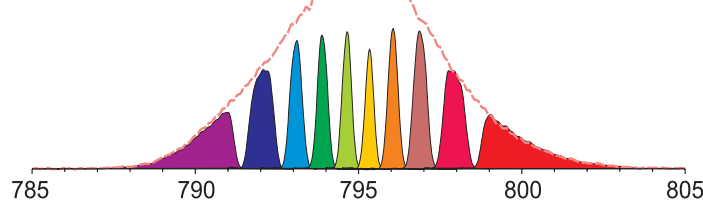
$$\Delta^2 \hat{E}_{P,i} \Delta^2 \hat{E}_{X,i} \quad < \hat{E}_{P,i} \hat{E}_{P,j} > < \hat{E}_{X,i} \hat{E}_{X,j} > < \hat{E}_{X,i} \hat{E}_{P,j} >$$

$$< \hat{E}_{X,i} \hat{E}_{X,j} > = \frac{1}{2} (\Delta^2 (\hat{E}_{X,i} + \hat{E}_{X,j}) - \Delta^2 \hat{E}_{X,i} - \Delta^2 \hat{E}_{X,j})$$

requires 55 homodyne measurements



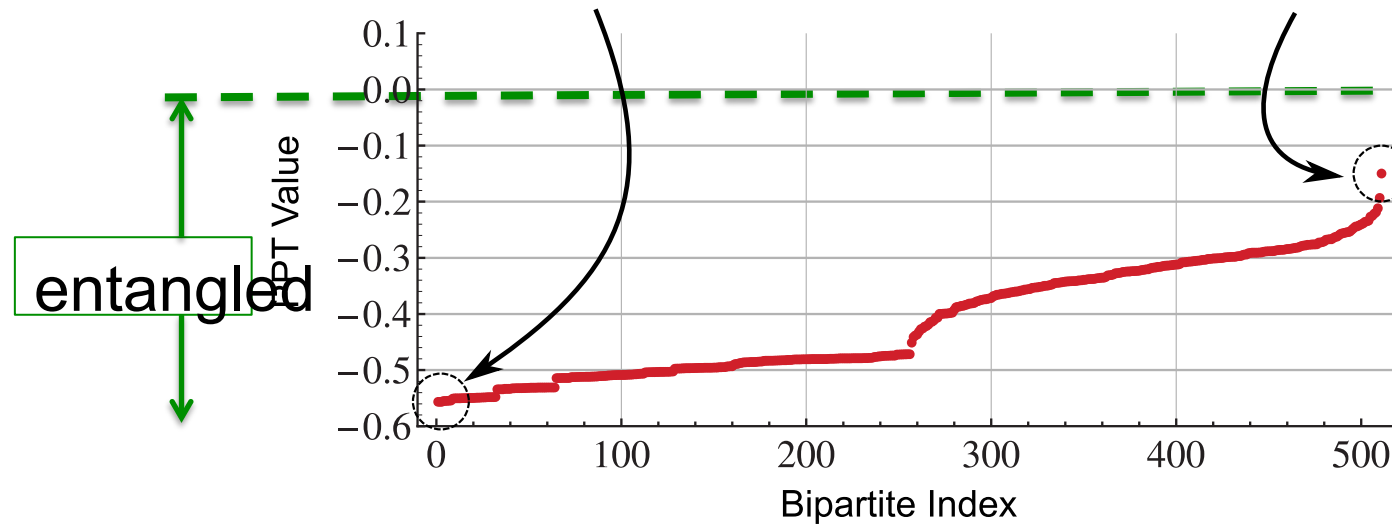
bi-partite entanglement ?



inspection of all 511 possible bipartitions with 10 pixels

"genuine" bi-partite entanglement ?

entanglement witness: **Positive Partial Transpose**



**all 511 bipartitions are
entangled !**

What about multipartite entanglement ?

Full multipartite entanglement of frequency comb Gaussian states

S. Gerke,^{1,*} J. Sperling,¹ W. Vogel,¹ Y. Cai,² J. Roslund,² N. Treps,² and C. Fabre²

¹*Arbeitsgruppe Theoretische Quantenoptik, Institut für Physik, Universität Rostock, D-18051 Rostock, Germany*

²*Laboratoire Kastler Brossel, Sorbonne Universités - UPMC, École Normale Supérieure, Collège de France, CNRS; 4 place Jussieu, 75252 Paris, France*

(Dated: September 25, 2014)

An analysis is conducted of the multipartite entanglement for Gaussian states generated by the parametric downconversion of a femtosecond frequency comb. Using a recently introduced method for constructing optimal entanglement criteria, a family of tests is formulated for mode decompositions that extend beyond the traditional bipartition analyses. A numerical optimization over this family is performed to achieve maximal significance of entanglement verification. For experimentally prepared 4, 6, and 10-mode states, full entanglement is certified for all of the 14, 202, and 115974 possible nontrivial partitions, respectively.

PACS numbers: 03.67.Mn, 42.50.-p, 03.65.Ud

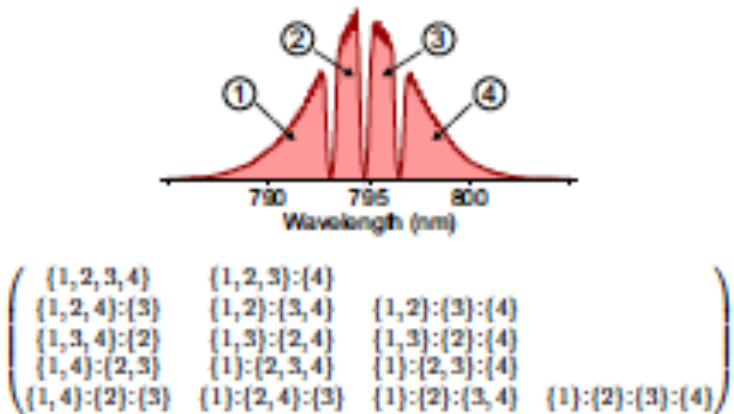


FIG. 1. (Color online) Structure of 4-mode state. The spectral components (top) and partitionings (bottom) are shown.

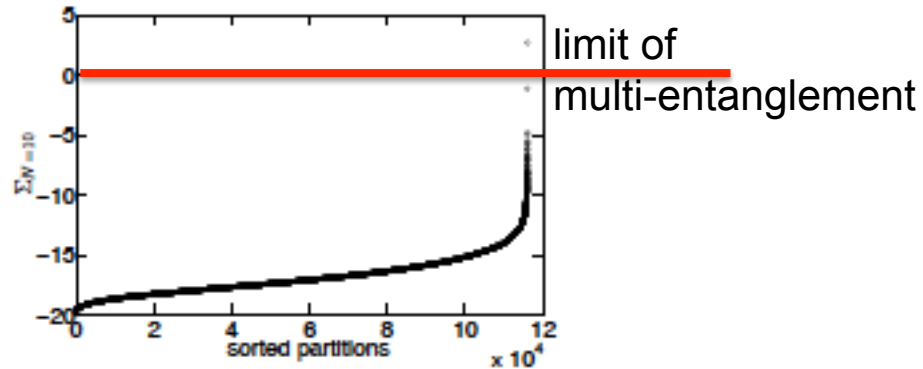


FIG. 3. The verified entanglement for all 115974 nontrivial partitions – sorted by significance Σ – for the 10-mode frequency-comb Gaussian state.

115 974 all entangled multipartitions !

experimental 20*20 covariance matrix:

x quadratures

p quadratures

$$\begin{pmatrix} 1.66 & 0.25 & 0.09 & 0.08 & -0.03 & -0.05 & -0.08 & -0.11 & -0.42 & -1.23 \\ 0.25 & 1.33 & 0.19 & 0.15 & 0.06 & -0.06 & -0.17 & -0.33 & -0.59 & -0.51 \\ 0.09 & 0.19 & 1.22 & 0.07 & -0.01 & -0.08 & -0.21 & -0.34 & -0.44 & -0.20 \\ 0.08 & 0.15 & 0.07 & 1.08 & -0.02 & -0.12 & -0.21 & -0.24 & -0.25 & -0.07 \\ -0.03 & 0.06 & -0.01 & -0.02 & 0.92 & -0.13 & -0.14 & -0.11 & -0.09 & 0.01 \\ -0.05 & -0.06 & -0.08 & -0.12 & -0.13 & 0.89 & -0.07 & 0.02 & 0.02 & 0.04 \\ -0.08 & -0.17 & -0.21 & -0.21 & -0.14 & -0.07 & 1.02 & 0.12 & 0.10 & 0.20 \\ -0.11 & -0.33 & -0.34 & -0.24 & -0.11 & 0.02 & 0.12 & 1.14 & 0.29 & 0.22 \\ -0.42 & -0.59 & -0.44 & -0.25 & -0.09 & 0.02 & 0.10 & 0.29 & 1.36 & 0.40 \\ -1.23 & -0.51 & -0.20 & -0.07 & 0.01 & 0.04 & 0.20 & 0.22 & 0.40 & 1.88 \end{pmatrix}$$

[0]

[0]

$$\begin{pmatrix} 1.66 & 0.25 & 0.09 & -0.02 & 0.04 & 0.00 & 0.01 & 0.09 & 0.39 & 1.19 \\ 0.25 & 1.33 & 0.19 & 0.05 & 0.13 & 0.12 & 0.14 & 0.28 & 0.50 & 0.53 \\ 0.09 & 0.19 & 1.22 & 0.17 & 0.21 & 0.28 & 0.32 & 0.37 & 0.39 & 0.26 \\ -0.02 & 0.05 & 0.17 & 1.31 & 0.35 & 0.38 & 0.37 & 0.33 & 0.26 & 0.12 \\ 0.04 & 0.13 & 0.21 & 0.35 & 1.38 & 0.47 & 0.43 & 0.31 & 0.22 & 0.10 \\ 0.00 & 0.12 & 0.28 & 0.38 & 0.47 & 1.42 & 0.42 & 0.30 & 0.19 & 0.10 \\ 0.01 & 0.14 & 0.32 & 0.37 & 0.43 & 0.42 & 1.34 & 0.27 & 0.21 & 0.08 \\ 0.09 & 0.28 & 0.37 & 0.33 & 0.31 & 0.30 & 0.27 & 1.30 & 0.22 & 0.15 \\ 0.39 & 0.50 & 0.39 & 0.26 & 0.22 & 0.19 & 0.21 & 0.22 & 1.36 & 0.40 \\ 1.19 & 0.53 & 0.26 & 0.12 & 0.10 & 0.10 & 0.08 & 0.15 & 0.40 & 1.88 \end{pmatrix}$$

$$Tr\rho^2 = 0.45 \pm 0.09$$

(3) mathematical search for uncorrelated modes

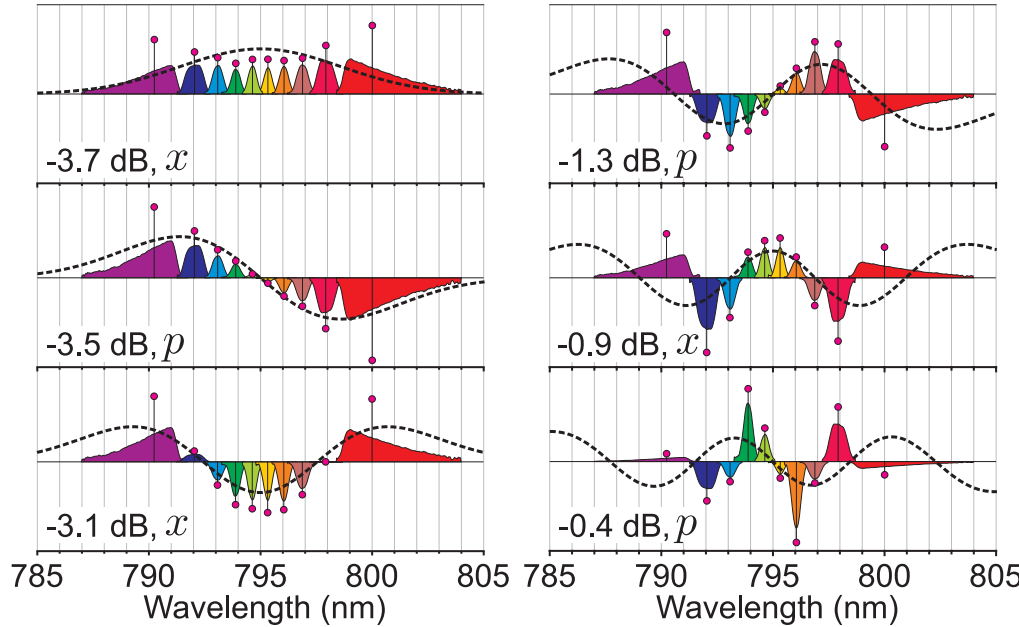
obtained by diagonalizing
the X or P measured covariance matrix

$\begin{pmatrix} 1.66 & 0.25 & 0.09 & 0.08 & -0.03 & -0.05 & -0.08 & -0.11 & -0.42 & -1.23 \\ 0.25 & 1.33 & 0.19 & 0.15 & 0.06 & -0.06 & -0.17 & -0.33 & -0.59 & -0.51 \\ 0.09 & 0.19 & 1.22 & 0.07 & -0.01 & -0.08 & -0.21 & -0.34 & -0.44 & -0.20 \\ 0.08 & 0.15 & 0.07 & 1.08 & -0.02 & -0.12 & -0.21 & -0.24 & -0.25 & -0.07 \\ -0.03 & 0.06 & -0.01 & -0.02 & 0.92 & -0.13 & -0.14 & -0.11 & -0.09 & 0.01 \\ -0.05 & 0.06 & 0.08 & 0.12 & 0.13 & 0.89 & -0.07 & 0.02 & 0.02 & 0.04 \\ -0.08 & -0.17 & -0.21 & -0.21 & -0.14 & -0.07 & 1.02 & 0.12 & 0.10 & 0.20 \\ -0.11 & -0.33 & -0.34 & -0.24 & -0.11 & 0.02 & 0.12 & 1.14 & 0.29 & 0.22 \\ -0.42 & -0.59 & -0.44 & -0.25 & -0.09 & 0.02 & 0.10 & 0.29 & 1.36 & 0.40 \\ -1.23 & -0.51 & -0.20 & -0.07 & 0.01 & 0.04 & 0.20 & 0.22 & 0.40 & 1.88 \end{pmatrix}$	[0]
$\begin{pmatrix} 1.66 & 0.25 & 0.09 & -0.02 & 0.04 & 0.00 & 0.01 & 0.09 & 0.39 & 1.19 \\ 0.25 & 1.33 & 0.19 & 0.05 & 0.13 & 0.12 & 0.14 & 0.28 & 0.50 & 0.53 \\ 0.09 & 0.19 & 1.22 & 0.17 & 0.21 & 0.28 & 0.32 & 0.37 & 0.39 & 0.26 \\ -0.02 & 0.05 & 0.17 & 1.31 & 0.35 & 0.38 & 0.37 & 0.33 & 0.26 & 0.12 \\ 0.04 & 0.13 & 0.21 & 0.35 & 1.38 & 0.47 & 0.43 & 0.31 & 0.22 & 0.10 \\ 0.00 & 0.12 & 0.28 & 0.38 & 0.47 & 1.42 & 0.42 & 0.30 & 0.19 & 0.10 \\ 0.01 & 0.14 & 0.32 & 0.37 & 0.43 & 0.42 & 1.34 & 0.27 & 0.21 & 0.08 \\ 0.09 & 0.28 & 0.37 & 0.33 & 0.31 & 0.30 & 0.27 & 1.30 & 0.22 & 0.15 \\ 0.39 & 0.50 & 0.39 & 0.26 & 0.22 & 0.19 & 0.21 & 0.22 & 1.36 & 0.40 \\ 1.19 & 0.53 & 0.26 & 0.12 & 0.10 & 0.10 & 0.08 & 0.15 & 0.40 & 1.88 \end{pmatrix}$	[0]

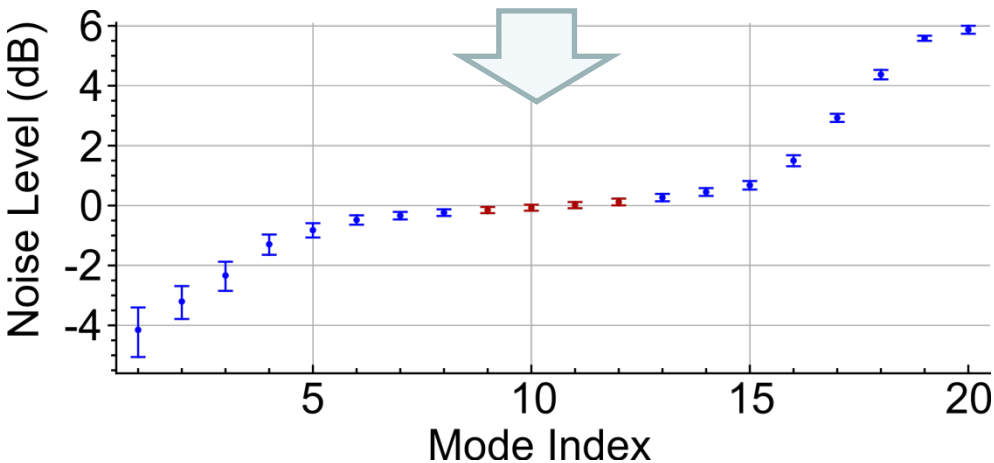
not always possible (non-commuting matrices)

search for mode basis change minimizing the off-diagonal terms

Eigenmodes or "supermodes" from 10 frequency bands



X and P matrix eigenvalues



8 modes contain
uncorrelated
squeezed vacuum states

the measured SPOPO output
is an
intrinsic 8-mode
non-classical state

Direct measurement of squeezing in the supermodes

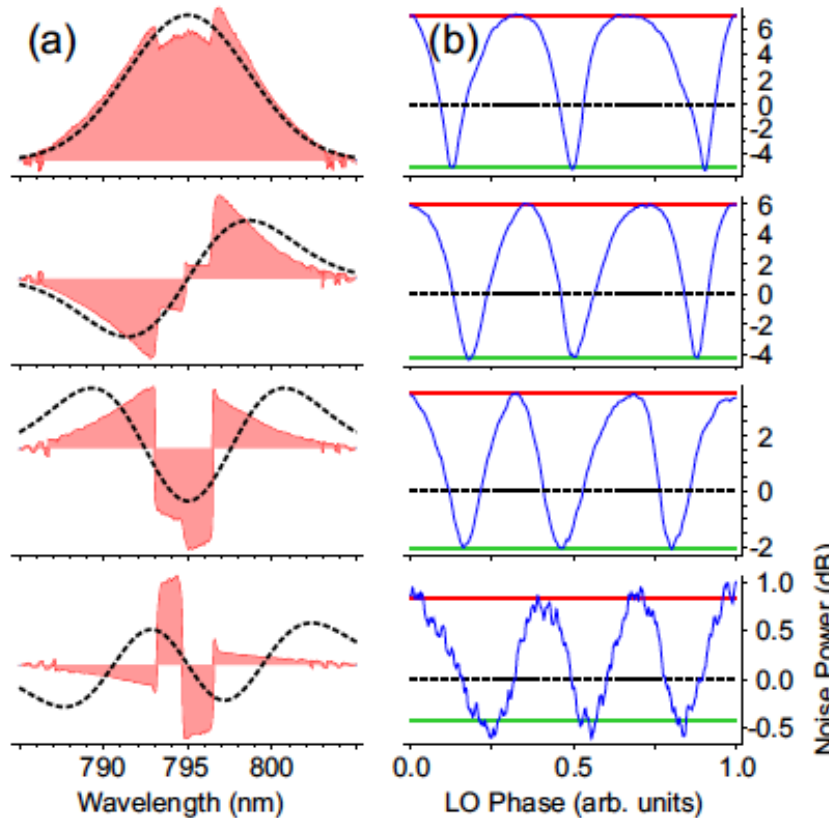
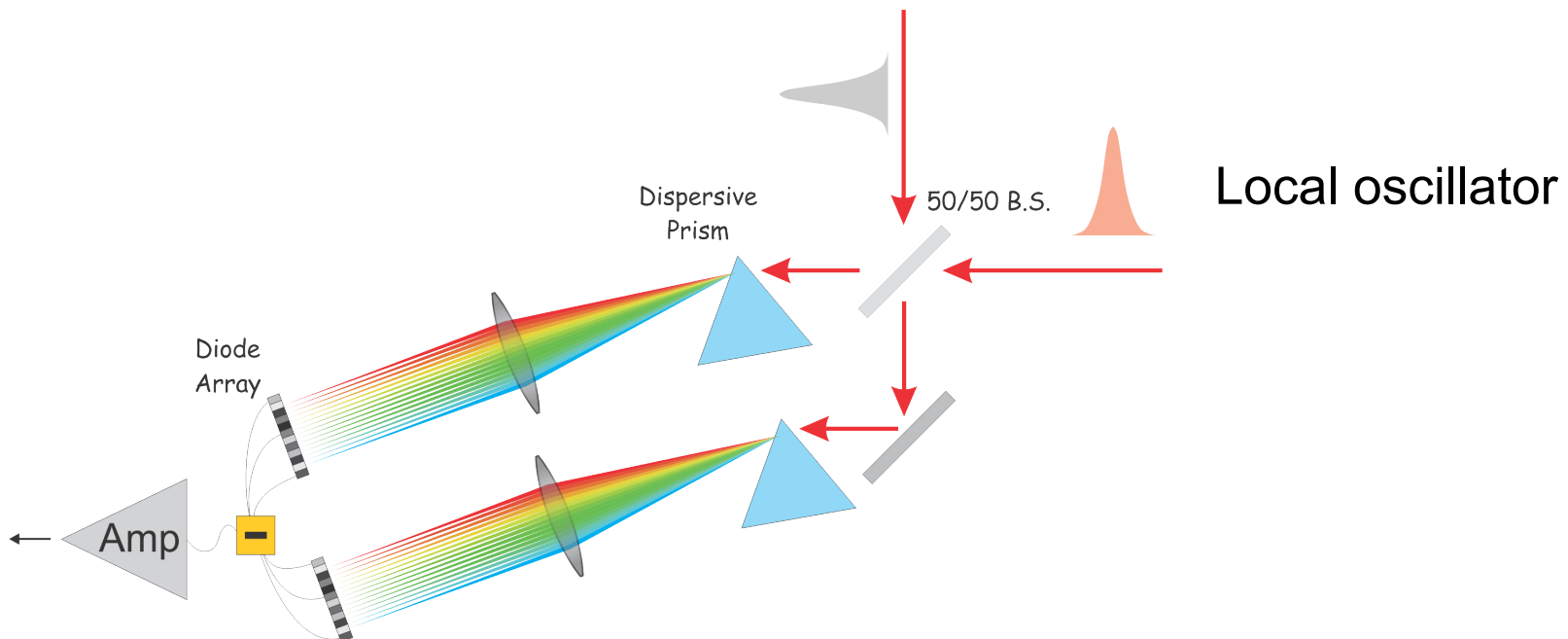


FIG. 7. (a) Retrieved experimental supermodes with the spectral gaps removed. The field of each supermode is measured with spectral interferometry. (b) Noise traces corresponding to each of the experimental supermodes.

same amounts of measured squeezing as determined by diagonalization

*One shot measurement
of the covariance matrix*

Multiplexed Homodyne Detection

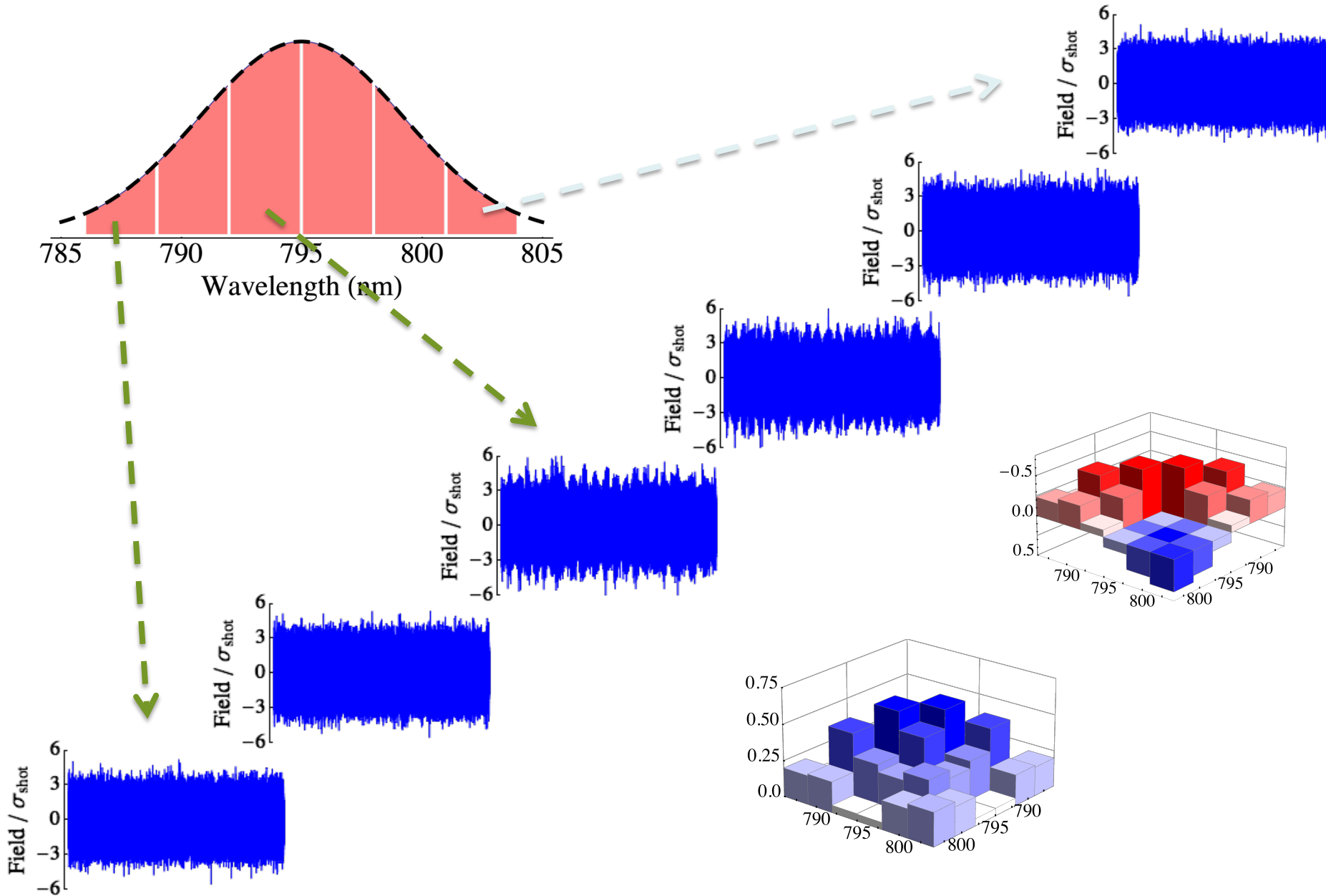


M. Beck, PRL 84 5748 (2000); S. Armstrong et al, Nat. Comm. 3, 1026 (2012).

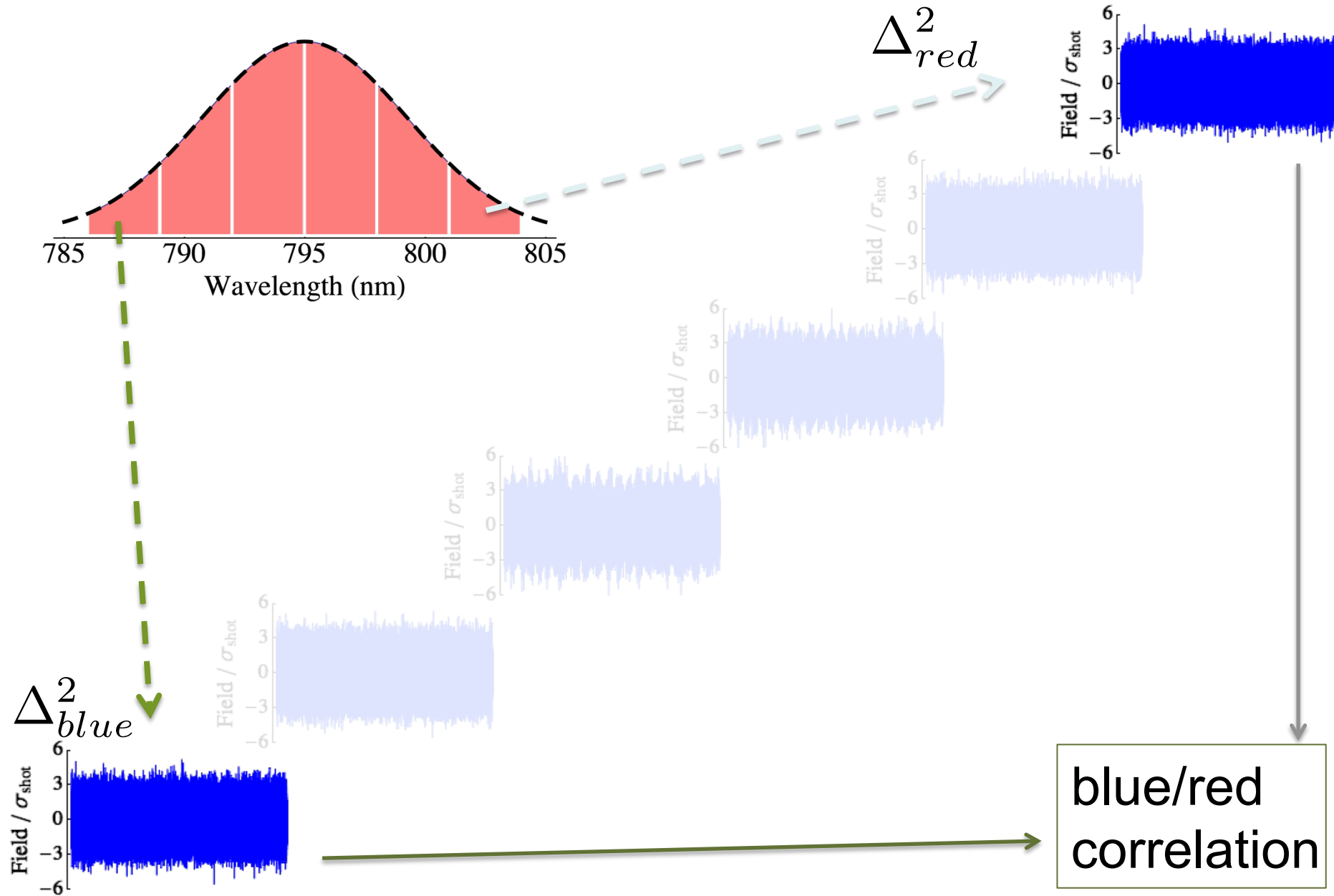
G. Ferrini et al New J Phys 15, 093015 (2013)

our experiment : array of 6 photodiodes

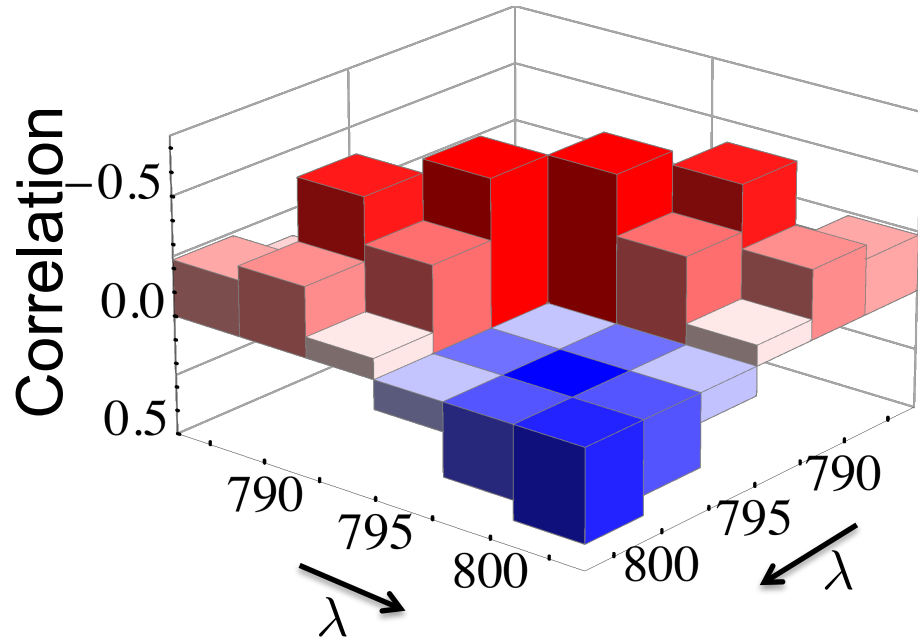
simultaneous detection of frequency band modes



simultaneous detection of frequency band modes

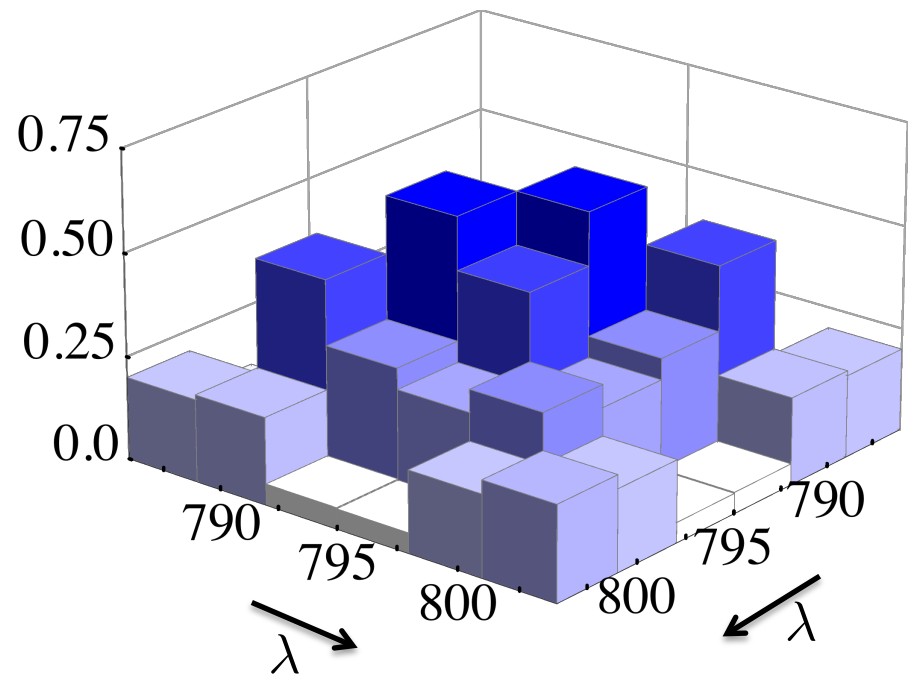


X and P covariance matrices

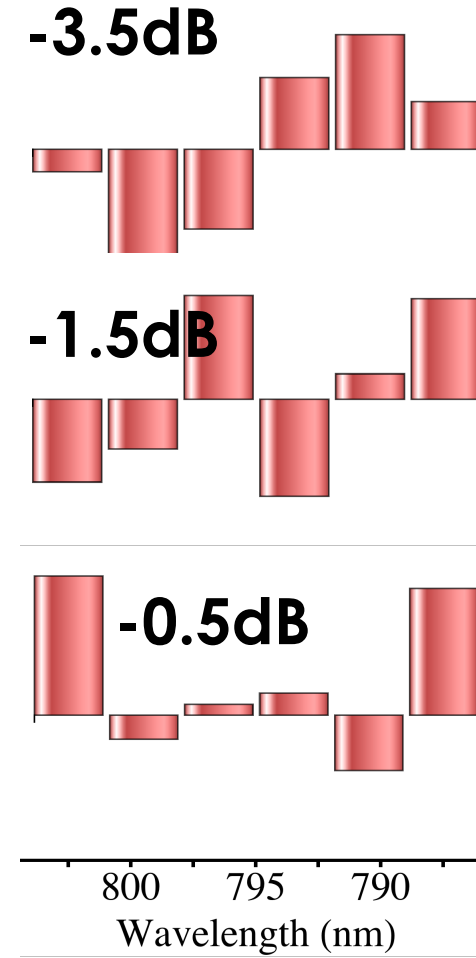


← **X Block Matrix**

P Block Matrix



diagonalization: squeezed eigenmodes

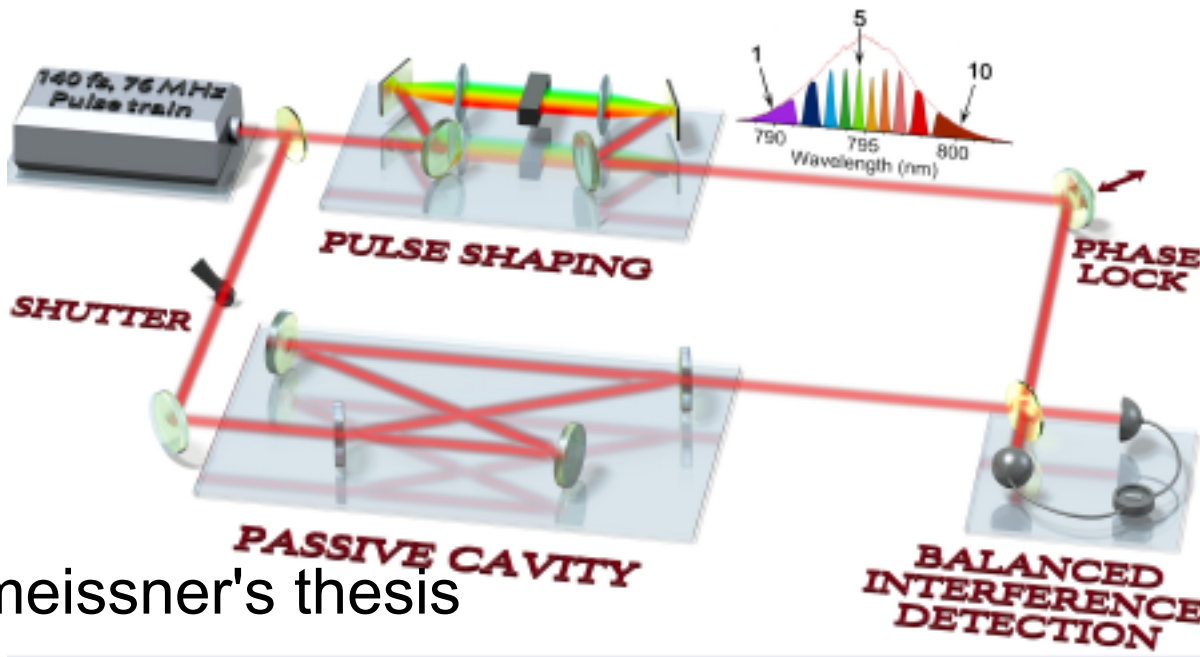


much faster data acquisition, and on a single quantum object

spectral analysis of phase and
amplitude fluctuations
of a mode-locked laser

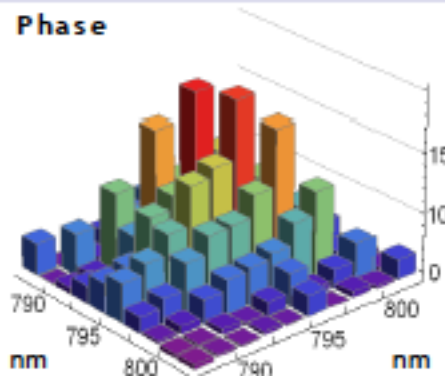
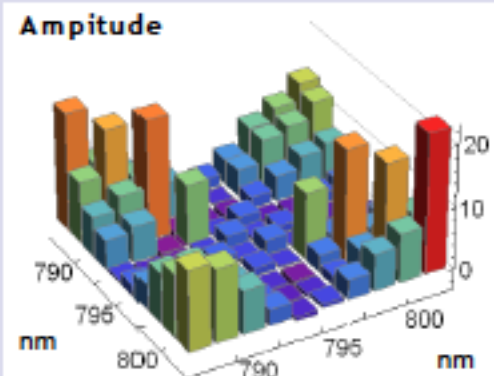
Thèse R. Shmeissner

study of the intensity and phase noise
of the frequency comb produced by the laser

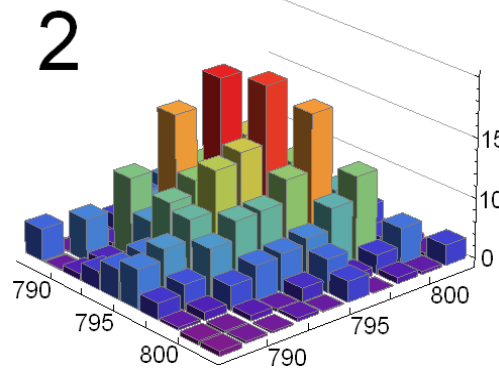
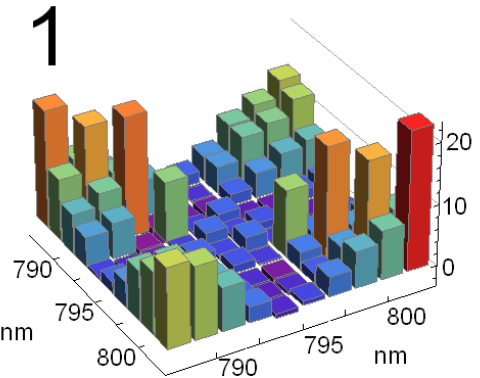


R. Schmeissner's thesis

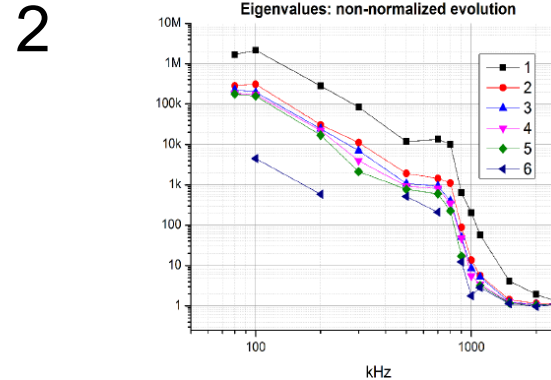
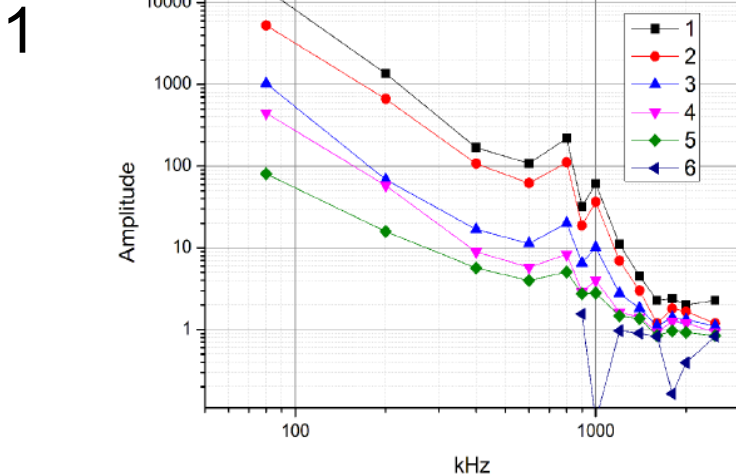
Noise covariance matrices for field properties:



Matrices de covariance des quadratures d'amplitude (1) et de phase (2)

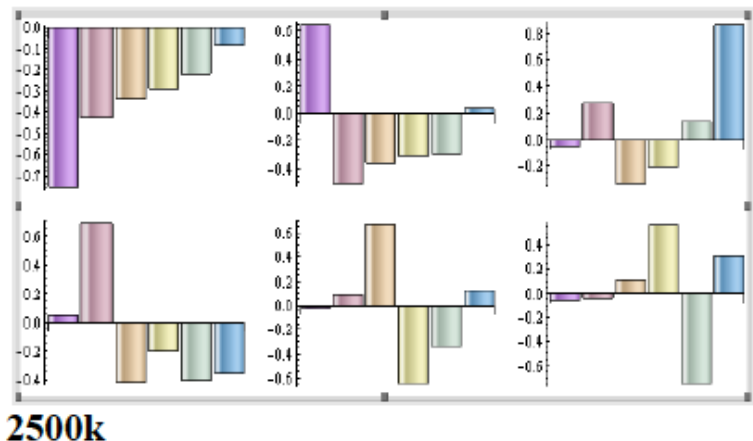


eigenvalues as a fonction of Fourier frequency



eigenstates as a fonction of Fourier frequency

1

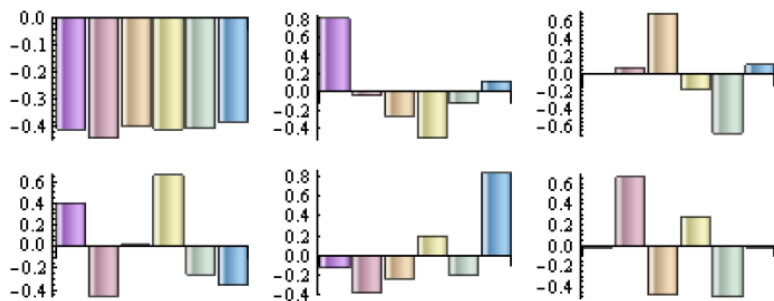


2500k

principal mode for amplitude noise

1100k

2



principal mode for phase noise
is mean field mode

$$E \simeq \langle E(r, t) \rangle e^{i\phi}$$

gives very rich information about the laser properties

extraction of cluster states
from the multimode state

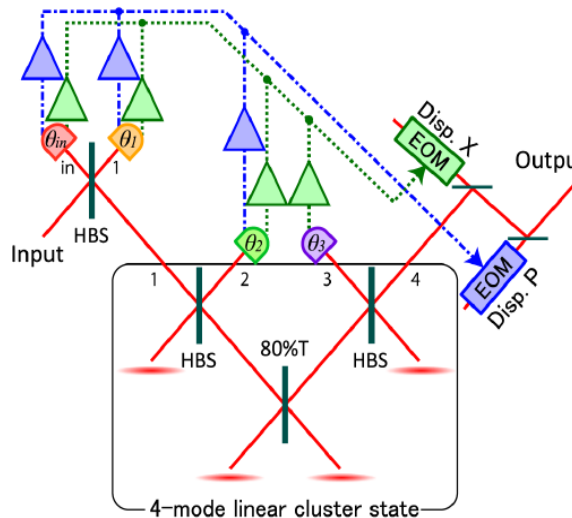
interesting states for one way quantum computing: the "cluster states"

example : the linear cluster state
can be generated from 4 squeezed modes by a basis change

$$U_{\text{lin}} = \begin{pmatrix} \frac{1}{\sqrt{2}} & \frac{1}{\sqrt{10}} & \frac{2i}{\sqrt{10}} & 0 \\ \frac{i}{\sqrt{2}} & -\frac{i}{\sqrt{10}} & \frac{2}{\sqrt{10}} & 0 \\ \frac{\sqrt{2}}{2} & -\frac{2}{\sqrt{10}} & \frac{i}{\sqrt{10}} & \frac{i}{\sqrt{2}} \\ 0 & -\frac{\sqrt{10}}{2} & \frac{\sqrt{10}}{2} & \frac{1}{\sqrt{2}} \\ 0 & -\frac{2i}{\sqrt{10}} & -\frac{1}{\sqrt{10}} & \frac{1}{\sqrt{2}} \end{pmatrix}$$

M. Yukawa, et al. Phys Rev A **78**, (2008), [Tokyo group](#).

generation by mixing
4 single mode
squeezed states

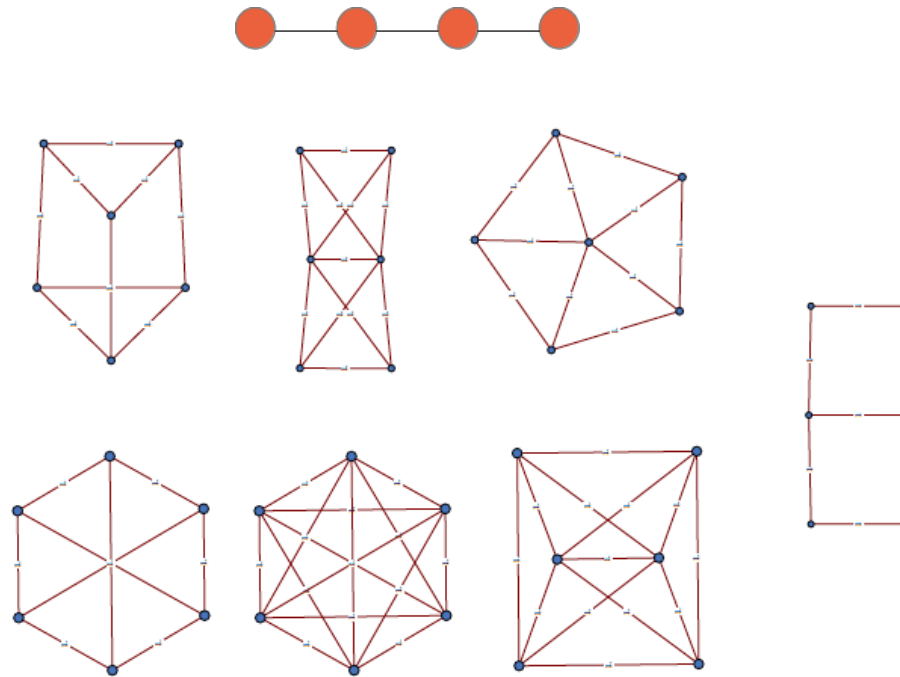


Implementation with frequency combs

$$\begin{aligned}
& \left[\begin{array}{c} M_1 \\ M_2 \\ M_3 \\ M_4 \end{array} \right] = \left(\begin{array}{cccc} \frac{1}{\sqrt{2}} & \frac{1}{\sqrt{10}} & \frac{2i}{\sqrt{10}} & 0 \\ \frac{i}{\sqrt{2}} & -\frac{i}{\sqrt{10}} & \frac{2}{\sqrt{10}} & 0 \\ 0 & -\frac{2}{\sqrt{10}} & \frac{i}{\sqrt{10}} & \frac{i}{\sqrt{2}} \\ 0 & -\frac{2i}{\sqrt{10}} & -\frac{1}{\sqrt{10}} & \frac{1}{\sqrt{2}} \end{array} \right) \times \left[\begin{array}{c} \text{Plot 1} \\ \text{Plot 2} \\ \text{Plot 3} \\ \text{Plot 4} \end{array} \right] \\
& = \left[\begin{array}{ccc} 0.38-0.05i & 0.29+0.36i & 0.29+0.37i \\ -0.05+0.38i & 0.36+0.29i & 0.37+0.29i \\ -0.13-0.57i & 0.53+0.05i & -0.45+0.26i \\ 0.57+0.13i & -0.05-0.53i & -0.27+0.45i \end{array} \right] \times \left[\begin{array}{c} \text{Plot 1} \\ \text{Plot 2} \\ \text{Plot 3} \\ \text{Plot 4} \end{array} \right]
\end{aligned}$$

measurements on cluster states nodes can be "extracted" using homodyne detection with appropriate LO

The "quality" of cluster states is characterized by "nullification" which can be evaluated by proper homodyne measurement



all these clusters "exist" in the SPOPO beam !

for measurement-based quantum computing

using cluster states

a **simultaneous measurement** of the nodes is necessary

Experiment in progress now in Paris

*optimization of modes in parameter
estimation*

Optical techniques are widely used to make
precise and sensitive estimations
of various parameters,

and in particular to position events in space and time

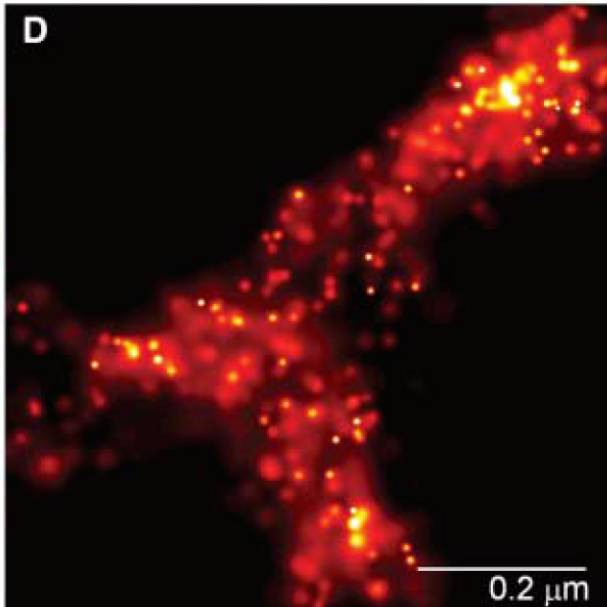
Measurements are carried out
by estimating **phase shifts**



or **time delays**

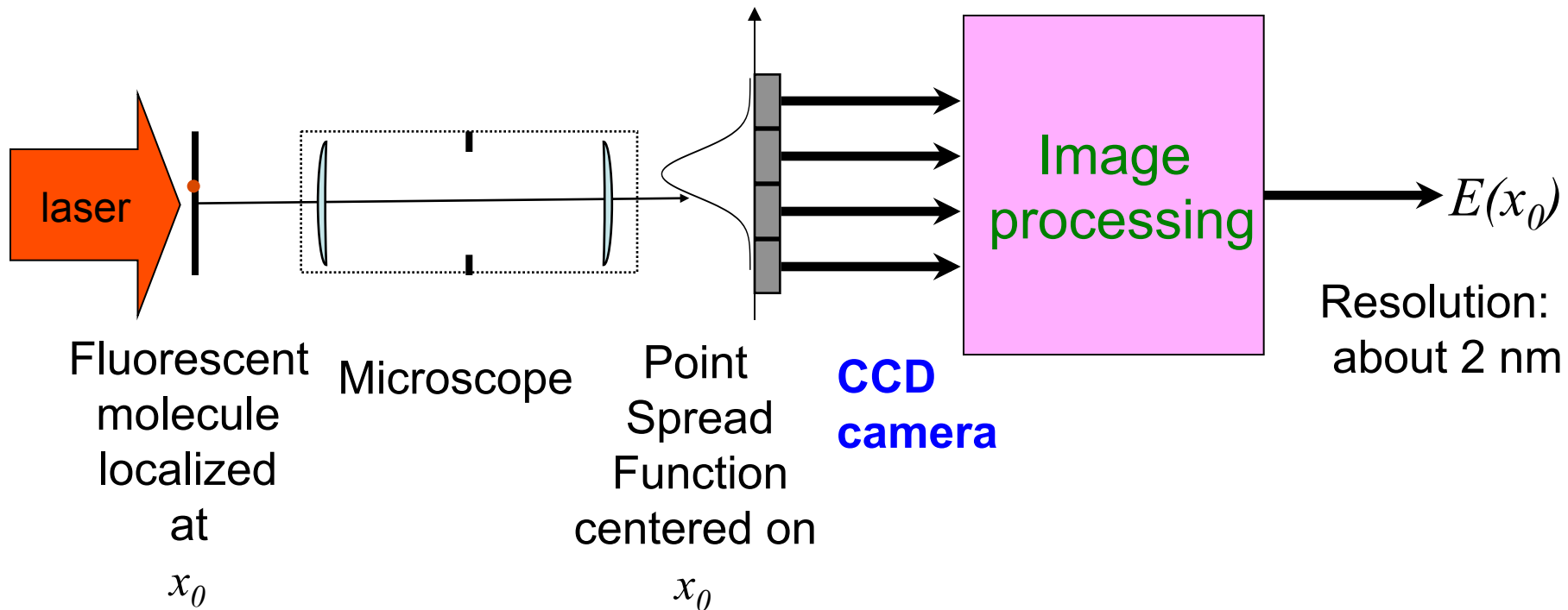


It is also possible to evaluate
transverse positions x_0, y_0
of fluorescent nano-objects

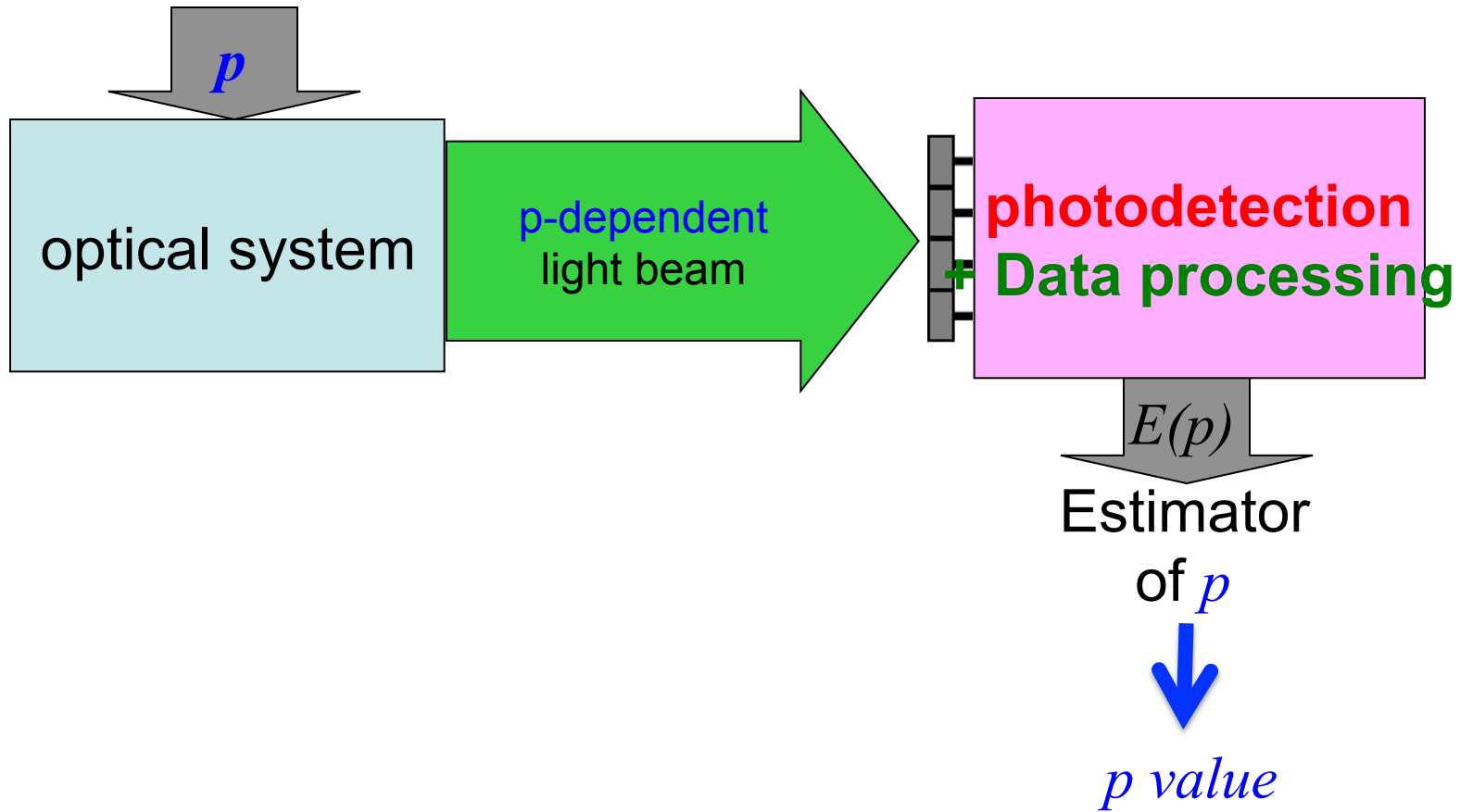


Imaging Intracellular Fluorescent
Proteins at Nanometer Resolution
E. Betzig et al Science 313 1642 (2006)

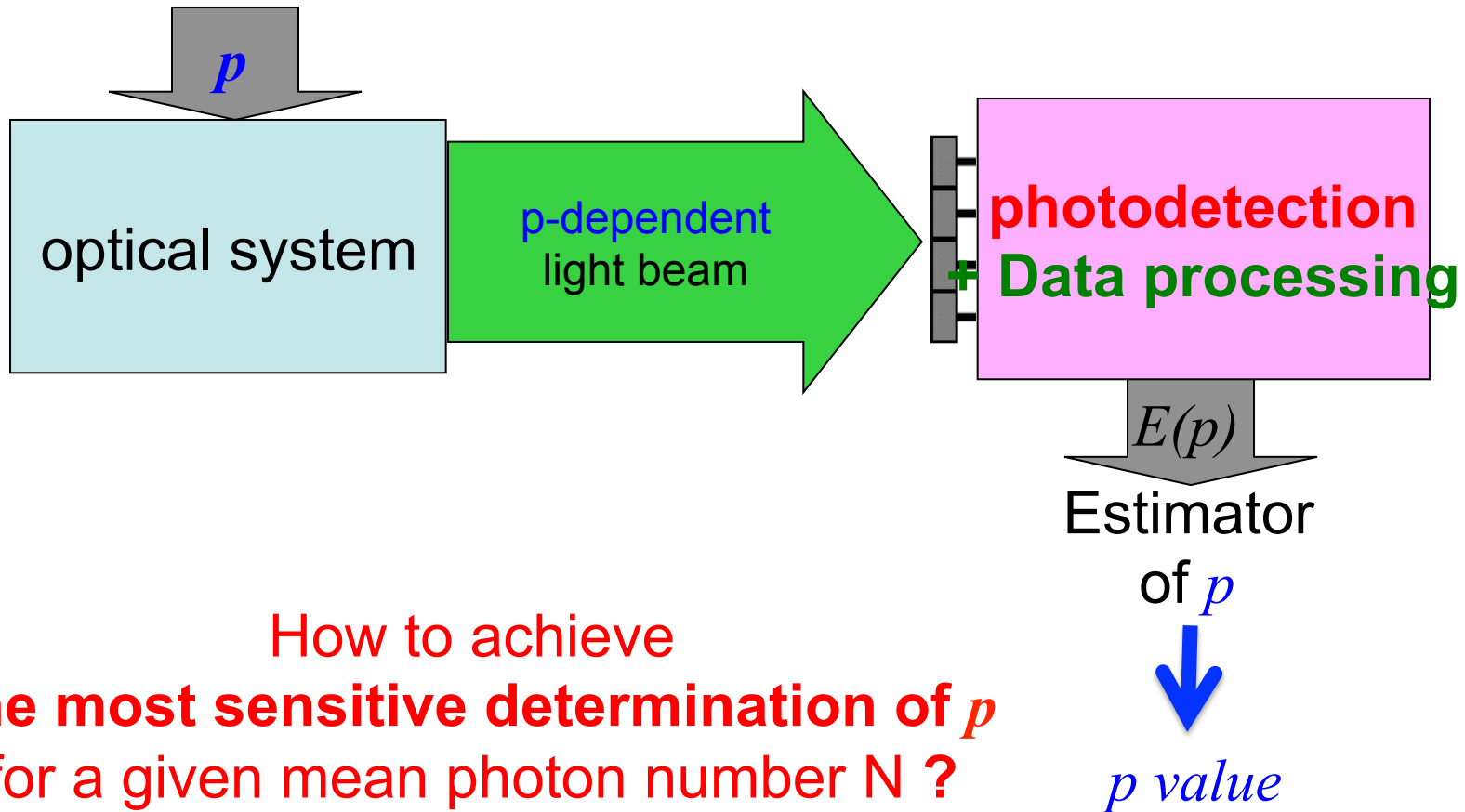
method for estimation of transverse position



General scheme for estimating a parameter p using information carried by light



General scheme for estimating a parameter p using information carried by light

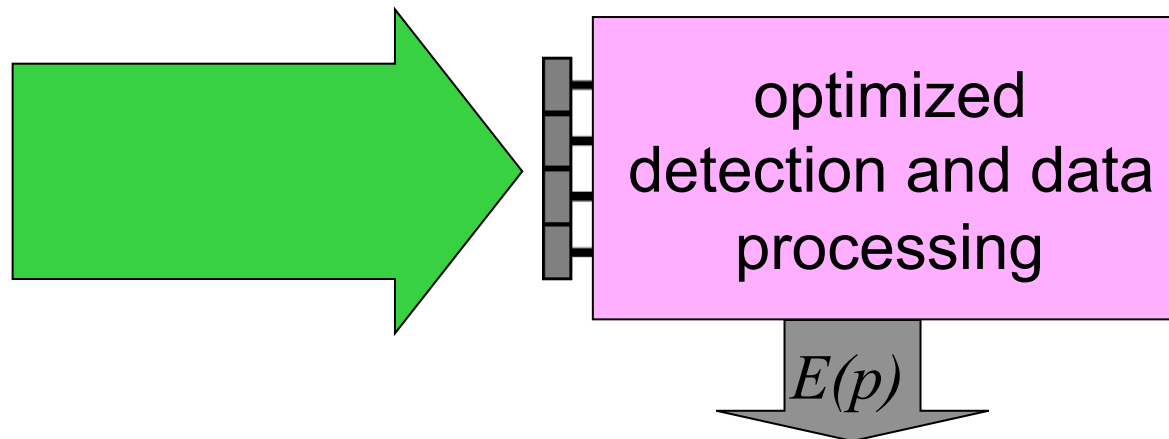


answer given by **Quantum Cramer Rao Bound**

Helstrom (1976), Caves, Braunstein (1994)

bound optimized over:

- all possible observables acting on light
- all possible data processing protocols

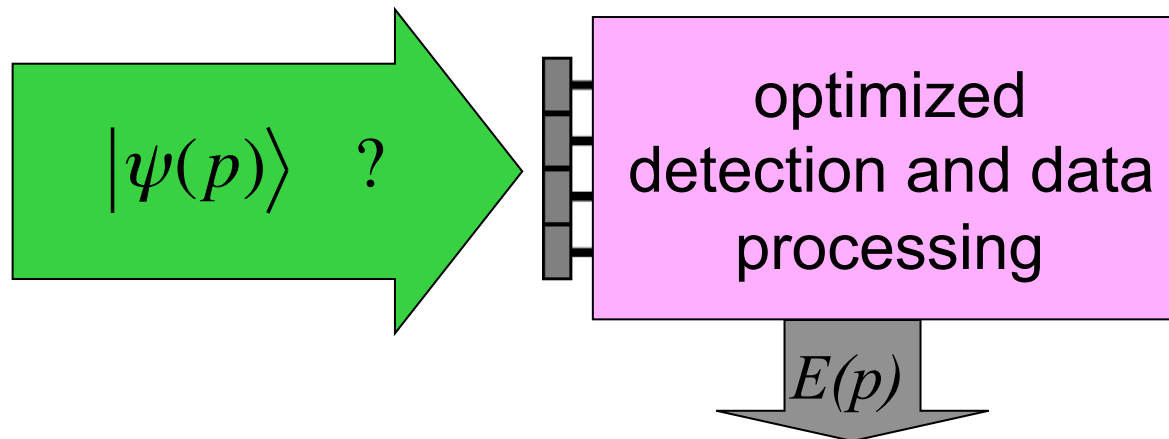


What remains to be chosen :

the quantum state of light

$$|\Psi(p)\rangle$$

used to carry the information in the experiment



possible choices ?

- **non-classical state of light**
squeezed, entangled, Fock, NOON ...

practical constraint :

state with large mean photon number N

because quantum limits scale as $1/N^x$

- **number of modes**
use of possible entanglement between modes
possible addition of the quantum effects of each mode
- **spatio-temporal shape of each mode**

novel aspect of the present approach

our choice : the multimode Gaussian pure state

includes a wide class of non-classical states

- single and multimode squeezed states
- multipartite quadrature entangled states
Einstein Podolsky Rosen paper state
- if it includes a coherent state in one mode:
 $\langle N \rangle = 10^{15}$ easy to reach
- readily available (12 dB squeezing)

excludes states which are « more quantum »,
like the NOON, or Fock states

- not available for very large $\langle N \rangle$ value
- hyper-sensitive to decoherence
- require complex photodetection schemes

Introduction of important modes

average mode :

spatio-temporal dependence of the average field value

$$u_{av}(x, y, t, p) = \frac{1}{\sqrt{N}} \langle \psi(p, t) | \hat{E}^{(+)}(x, y) | \psi(p, t) \rangle$$

$$u_{av}(x, y, t, p_0 + \delta p) = u_{av}(x, y, t, p_0) + \delta p \frac{\partial u_{av}}{\partial p} \Big|_{p_0}$$

detection mode :

sensitivity of illumination mode to the parameter variation

$$u_{det}(x, y, t) = p_c \frac{\partial u_{av}}{\partial p} \Big|_{p=p_0}$$

normalizing factor

Quantum Cramer Rao bound for Gaussian pure states

p-sensitivity

expression in the high N limit:

$$\Delta p_{QCRb} = \frac{p_c}{2\sqrt{N}} \Delta_{\text{det}}$$

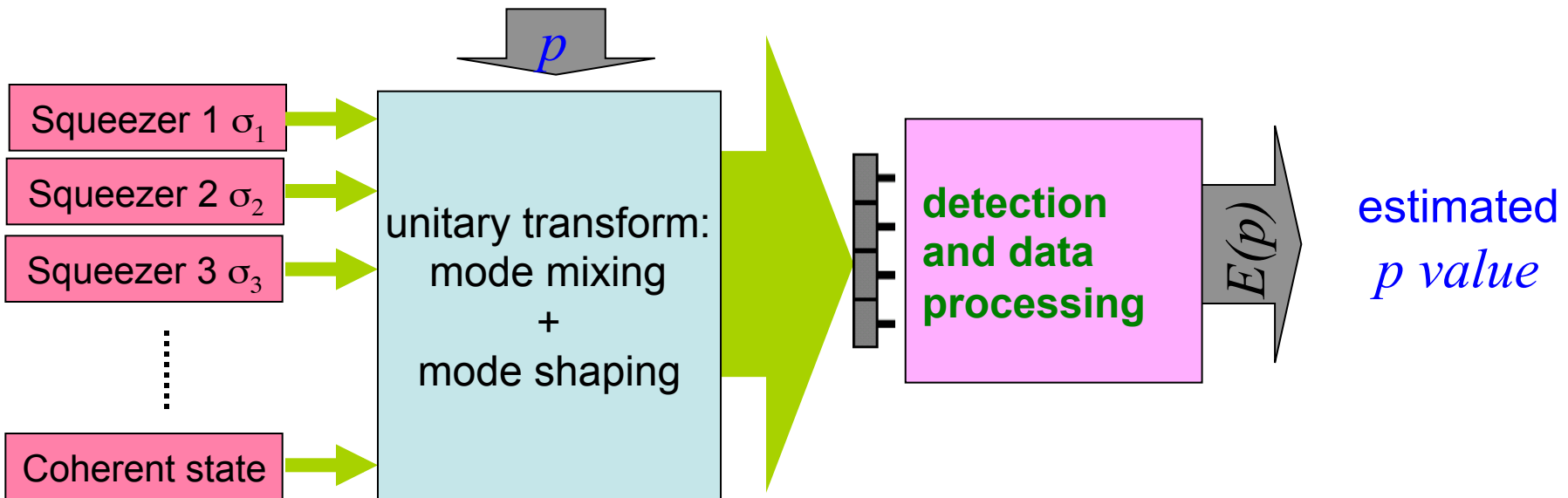
« shot noise »

noise term

Noise in the detection mode u_{det}
normalized to shot noise

value independent
of the fluctuations of all modes orthogonal to u_{det}

Quantum Cramér Rao bound using **minimal** non-classical Gaussian resources



The lowest Quantum Cramér Rao bound is obtained:

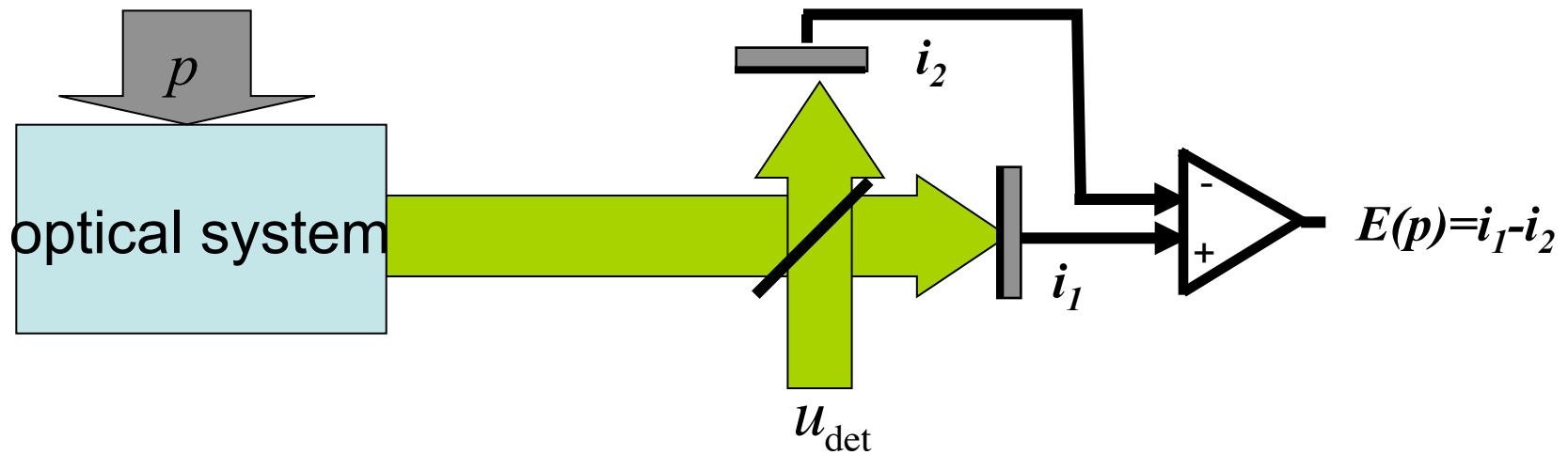
- when the most squeezed beam available is put in the detection mode
- when there are no correlations between the detection mode and the other modes

Conclusions for the experimentalist

- **Multisqueezing does not help**
squeezing is not « additive »
- **Entanglement does not help**
it actually reduces squeezing in the right mode
- **Squeeze one mode but the right one**
maximum possible single mode squeezing
in the detection mode

How to make an estimation at the QCR bound ?

use **homodyne detection**
with detection mode as a local oscillator

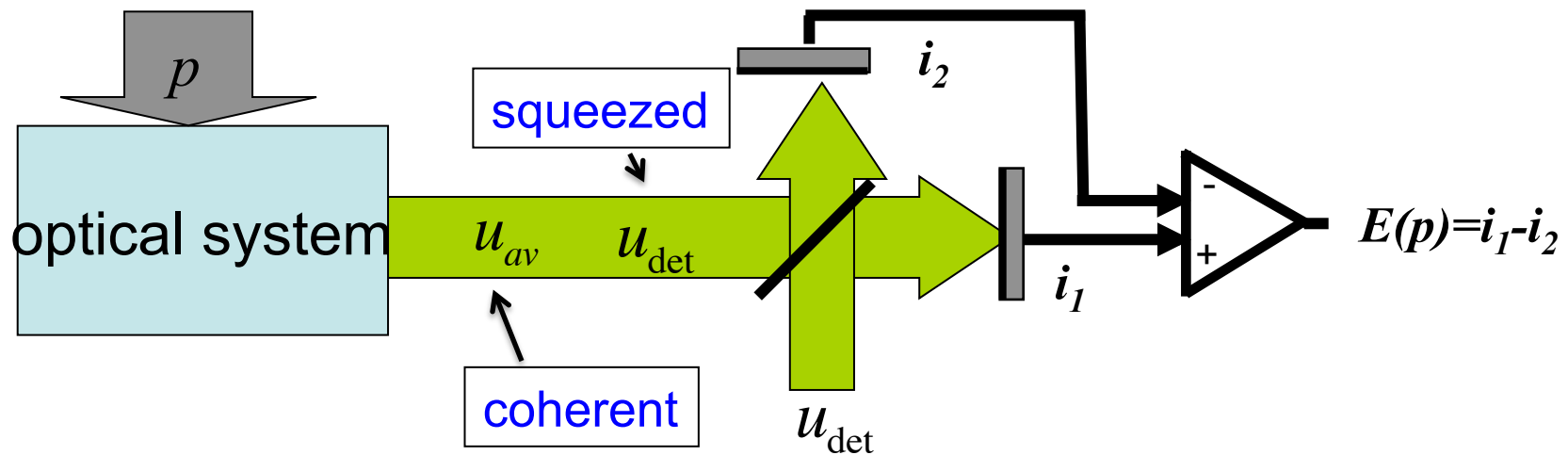


no other measurement starting from u_{av}
(given mean field) can do better

How to make an optimized estimation beyond shot noise ?

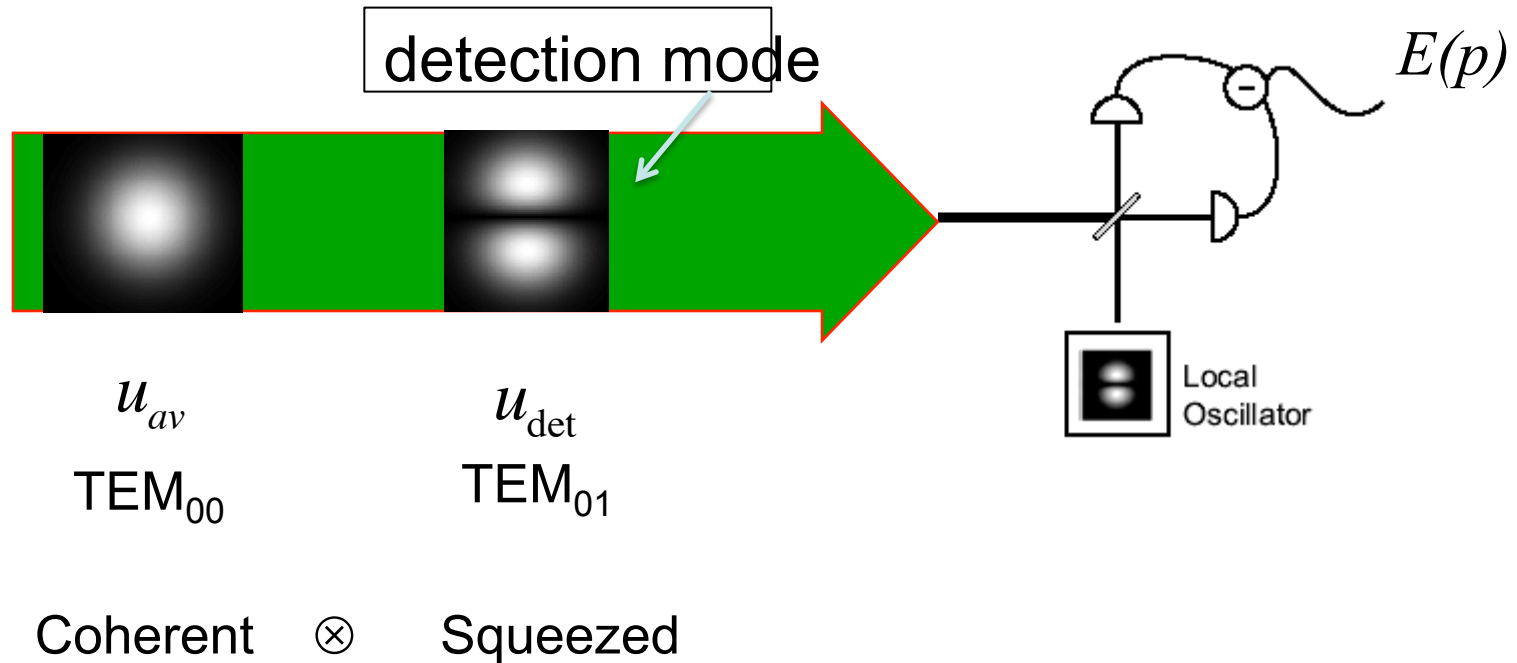
use a light beam made of:

- coherent state in average mode u_{av}
- squeezed vacuum state in detection mode u_{det}



Optimized estimation of transverse position

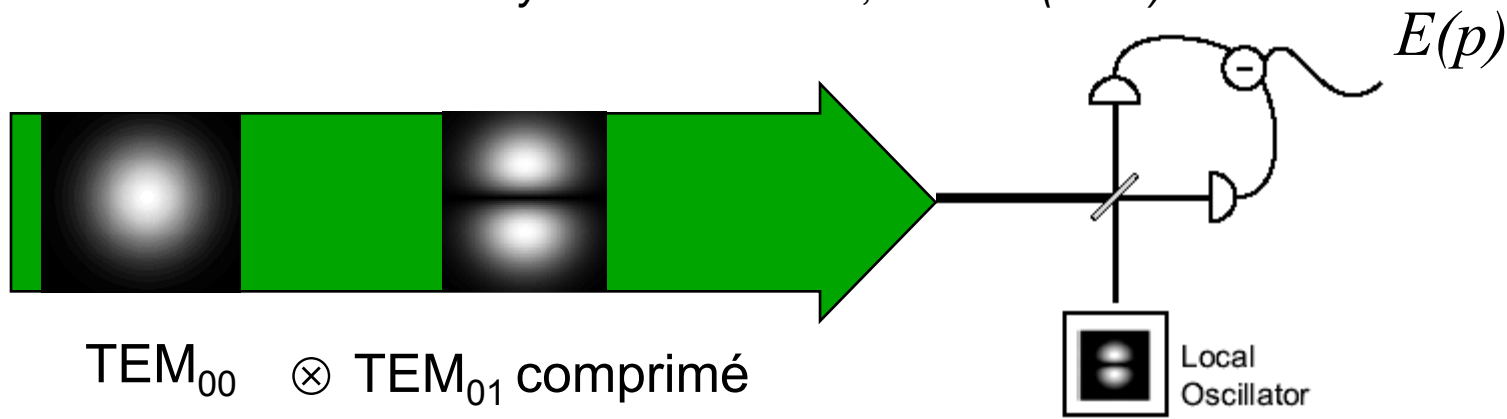
TEM₀₀ beam :



Experiment

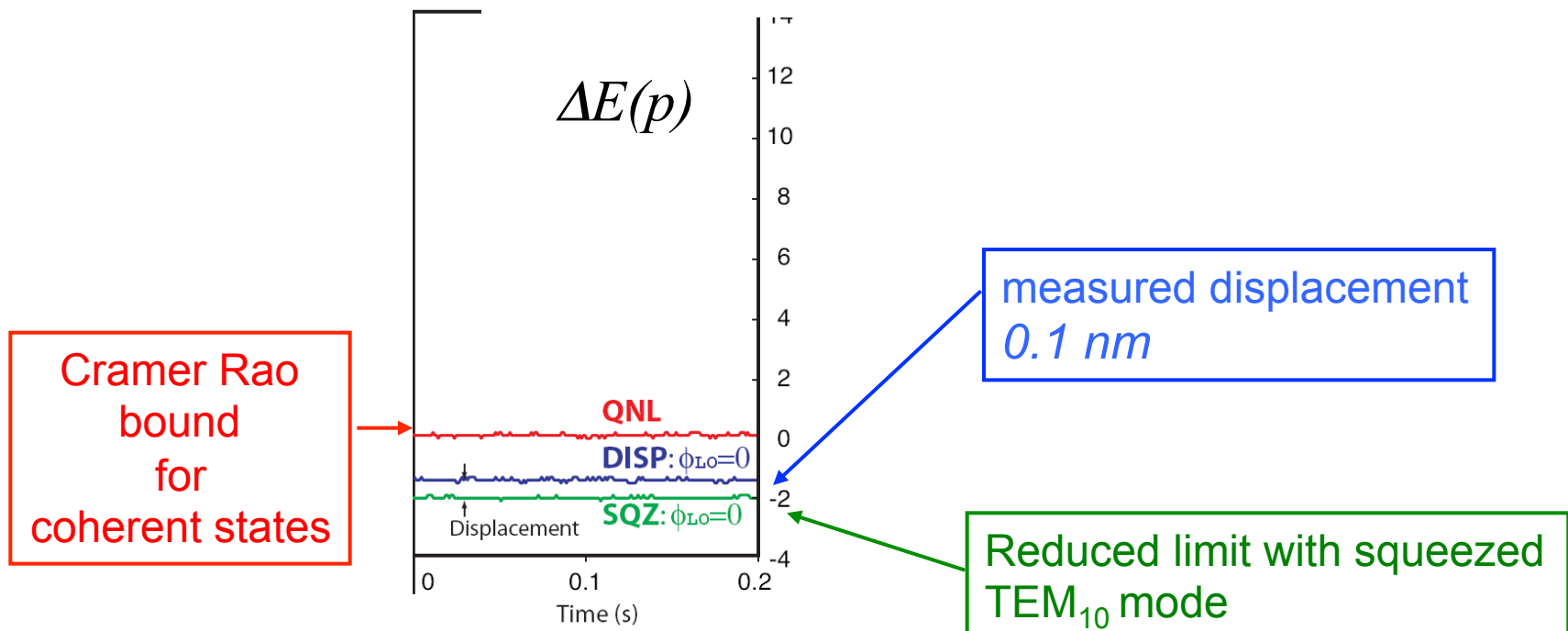
(collaboration ANU Canberra LKB Paris)

M. Lassen et al. Phys. Rev Letters 98, 083602 (2007)

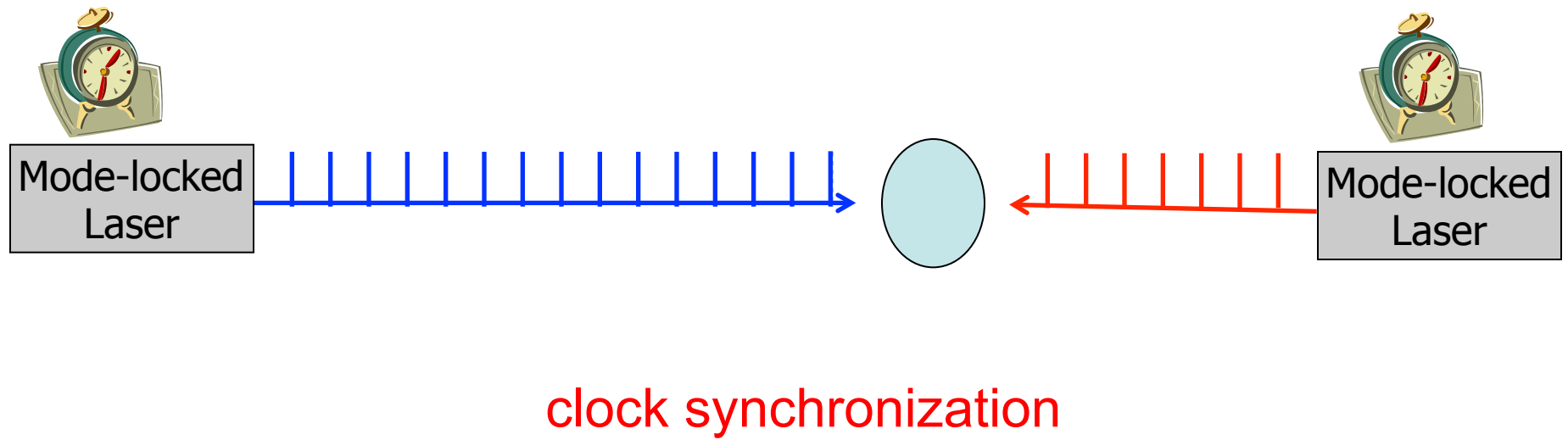


$\text{TEM}_{00} \otimes \text{TEM}_{01}$ comprimé

Local
Oscillator

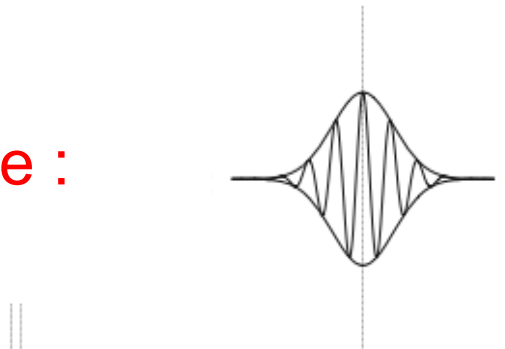


Optimized estimation of time delays



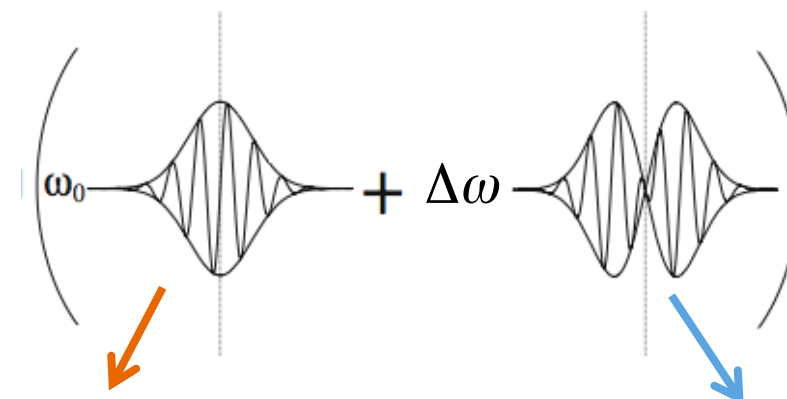
*B. Lamine, C. Fabre, N. Treps,
Phys. Rev. Letters 101 123601 (2008)*

average mode :



HG0

detection mode :



Carrier displacement :
phase
HG0

Envelope
displacement : time
of flight
HG1

Quantum Cramer Rao bound

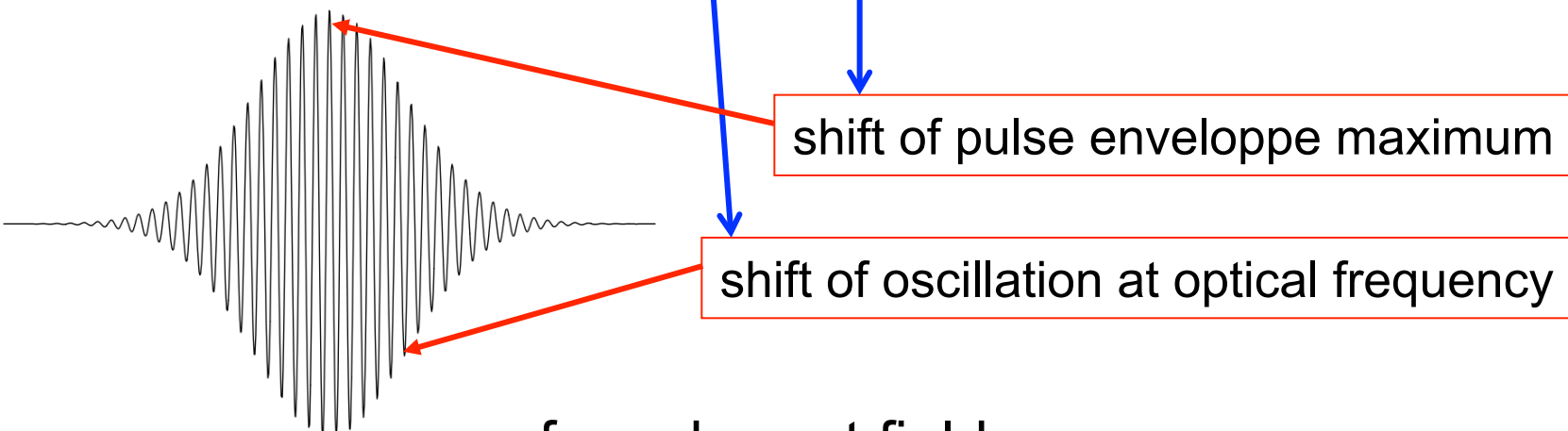
N : total number of photons

$$(\Delta t)_{S-CRb} = \frac{1}{\sqrt{N}} \frac{1}{2\sqrt{\omega_0^2 + \Delta\omega^2}} \Sigma_{\text{det}}$$

ω_0 : mean frequency

$\Delta\omega$: frequency spread

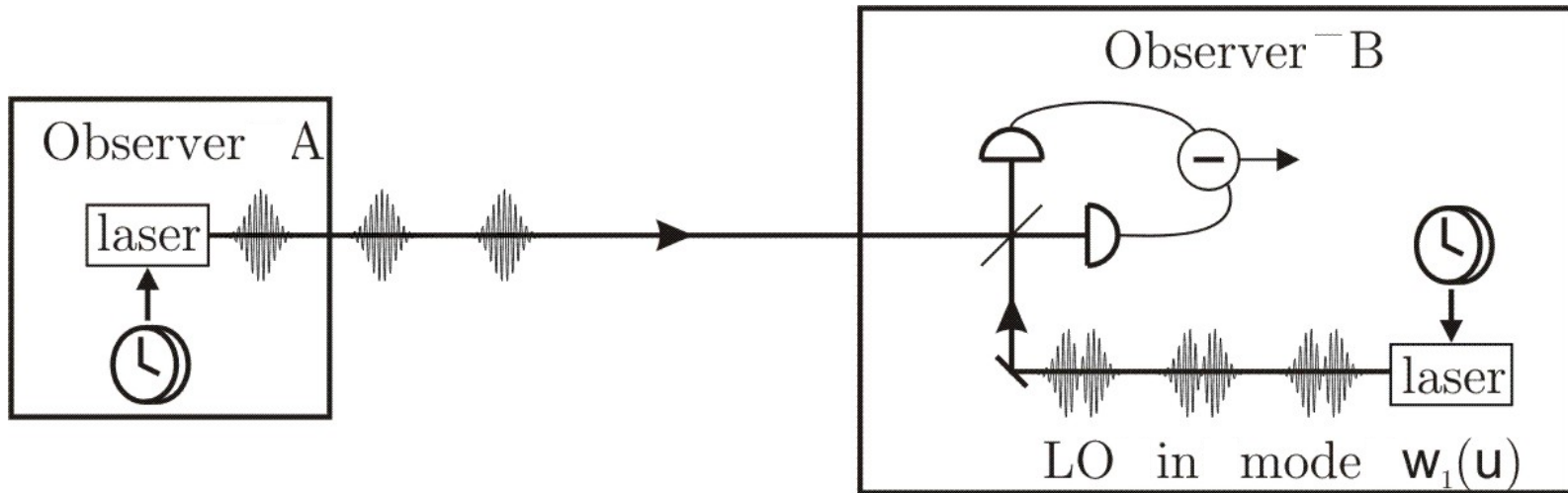
Σ_{det} : noise in detection mode



for coherent field :

10mw, 10fs, 100MHz, 1s integration
time $(\Delta u)_{crb}^{coherent} = 5.10^{-23}s$

Optimal measurement reaching the Cramer Rao bound



Local Oscillator in detection mode

to squeeze the detection mode :

use **quantum frequency comb** generated by a synchronously pumped OPO

